

# Thermal noise and correlations in photon detection

Jonas Zmuidzinas

The standard expressions for the noise that is due to photon fluctuations in thermal background radiation typically apply only for a single detector and are often strictly valid only for single-mode illumination. I describe a technique for rigorously calculating thermal photon noise, which allows for arbitrary numbers of optical inputs and detectors, multiple-mode illumination, and both internal and external noise sources. Several simple examples are given, and a general result is obtained for multimode detectors. The formalism uses scattering matrices, noise correlation matrices, and some fundamentals of quantum optics. The covariance matrix of the photon noise at the detector outputs is calculated and includes the Hanbury Brown and Twiss photon-bunching correlations. These correlations can be of crucial importance, and they explain why instruments such as autocorrelation spectrometers and pairwise-combined interferometers are competitive (and indeed common) at radio wavelengths but have a sensitivity disadvantage at optical wavelengths. The case of autocorrelation spectrometers is studied in detail.

© 2003 Optical Society of America

OCIS codes: 270.2500, 350.1270, 030.4280, 030.5290.

## 1. Introduction

The sensitivities of astronomical instruments are often limited primarily by the fluctuations of the background radiation received by the detectors. This is especially true for ground-based instruments in the millimeter through infrared wavelength bands, for which the dominant thermal backgrounds are contributed by the emission from the telescope and the atmosphere. At short wavelengths (e.g., optical or near IR), the background photon counts follow a Poisson distribution, and the fluctuations are given by  $\sqrt{N}$  where  $N$  is the mean number of photons received. It is well known that this Poisson distribution holds only in the case that the mean photon mode occupation number is small,  $n \ll 1$ . For a thermal blackbody background, the occupation number is given by the Bose–Einstein formula,  $n_{\text{th}}(\nu, T) = [\exp(h\nu/kT) - 1]^{-1}$ , so the opposite classical limit  $n \gg 1$  is the usual situation at longer wavelengths for which  $h\nu \ll kT$ . When  $n \gg 1$ , the photons do not arrive independently according to a Poisson process but instead are strongly bunched, and the fluctuations are of order  $N$

instead of  $\sqrt{N}$ . This is why radio astronomers use the Dicke equation<sup>1</sup> to calculate sensitivities, which states that the noise is proportional to the background power rather than its square root. In addition, as first shown by Hanbury Brown and Twiss,<sup>2</sup> bunching can produce noise correlations between different detectors.

Thus, it is interesting to explore the connection between the sensitivity expressions used in optical and radio astronomy.<sup>3</sup> This interest is not purely academic; the behavior of noise in these two regimes can determine the relative sensitivities of various instrument architectures. For example, a topic of great current interest is the possibility of measuring the polarization of the cosmic microwave background.<sup>4</sup> Current cosmic microwave background intensity anisotropy instruments use a wide variety of techniques, drawn from both radio and optical astronomy, including coherent and direct detection, as well as single-aperture focal plane array imaging and interferometric aperture synthesis imaging. New variations of these techniques are emerging, such as the combination of interferometry with direct detection. It is also interesting to note that CMB experiments often operate in the crossover regime,  $n \sim 1$ .

The usual example used to illustrate the distinction between the radio and the optical regimes is the use of coherent receivers, which are subject to a quantum noise limit of one photon of added noise per mode.<sup>5</sup> This is not considered important for radio astronomy ( $n \gg 1$ ) but would be a very large penalty in the optical ( $n \ll 1$ ) band.<sup>6</sup> Another example that

---

J. Zmuidzinas (jonas@submm.caltech.edu) is with the Division of Physics, Mathematics, and Astronomy, 320-47, California Institute of Technology, 1200 East California Boulevard, Pasadena, California 91125-0000.

Received 13 November 2002; revised manuscript received 15 May 2003.

0003-6935/03/254989-20\$15.00/0

© 2003 Optical Society of America

I study in detail is the autocorrelation spectrometer, which is common at radio wavelengths but does not offer competitive sensitivity for optical spectroscopy. An analogous situation occurs in the design of spatial interferometric arrays for which the pairwise combination of telescopes used at radio wavelengths is indeed appropriate when  $n \gg 1$  but suffers from an additional noise penalty for the low-background ( $n \ll 1$ ) direct detection case.<sup>7</sup> As we shall see, the photon noise correlations among the various detectors play an essential role in determination of the sensitivities of autocorrelators and interferometers.

The sensitivity limitation that is due to thermal radiation fluctuations has been discussed numerous times in the literature over the past 60 years.<sup>8–20</sup> The experimental demonstration of photon correlations (the Hanbury Brown and Twiss effect)<sup>2,21–23</sup> stimulated a great deal of interest and effort<sup>13,14,22,24–32</sup> to understand these correlations theoretically and to resolve discrepancies with previous expressions for thermal photon fluctuations derived from thermodynamic arguments (the Einstein–Fowler relation).<sup>13</sup> This work led to the following equation (which is rederived in this paper) for the  $1\sigma$  uncertainty in the optical power after an integration time  $\tau$ :

$$\sigma_P = \frac{h\nu\Delta\nu}{\eta\sqrt{\Delta\nu\tau}} [\eta n_0(1 + \eta n_0)]^{1/2}, \quad (1)$$

when thermal radiation with a photon occupation number  $n_0$  is detected by use of a noiseless single-mode detector with quantum efficiency  $\eta$  and optical bandwidth  $\Delta\nu$ . Here, the first term in the square root gives the usual  $\sqrt{N}$  Poisson fluctuations, whereas the second term, important only when  $\eta n_0$  is of the order of unity or larger, accounts for the photon correlations or bunching and provides the transition to the Dicke radiometer equation in the  $\eta n_0 \gg 1$  limit. The additional factor of  $\eta$  on the bunching term is crucial but was missing prior to the work of Hanbury Brown and Twiss.<sup>2</sup> This factor is needed to recover the Dicke limit properly and also to understand the photon correlation experiments quantitatively. However, the correct expression for the bunching term has been questioned<sup>19</sup> for the case in which the detector is illuminated by more than one spatial mode.

Here I present a complete theory of thermal noise in photon detection, which allows for multiple detectors and spatial modes and also includes the noise correlations between detectors. In Section 2, I develop the noise theory by use of a straightforward application of the concepts of quantum optics. The theory is applied to both single-mode and multimode detectors in Sections 3 and 4. In Section 5 the theory is used to study the sensitivity of autocorrelation spectrometers.

## 2. Thermal Photon Noise Theory

### A. Scattering Matrix Description of Optical Components and Systems

We use a scattering matrix description of optical systems<sup>7</sup> and use quantum operators in place of classical field amplitudes. The use of scattering matrices allows us to describe thermal noise in linear electrical networks equally well. This is quite useful, since instruments built for the millimeter or submillimeter wavelength bands (the transition region between radio and infrared) often use a combination of optical components (such as lenses and mirrors) as well as microwave circuit techniques (horns, waveguides, transmission lines, and filters). Also, the scattering matrix approach is particularly well suited for describing single-mode optical fibers and integrated optical devices. In the low-frequency Rayleigh–Jeans limit,  $h\nu \ll k_B T$ , the theory reproduces the standard results for thermal noise in circuits.<sup>33–36</sup>

Any arbitrary optical element or an entire optical system, excluding the detectors, can be described by a classical scattering matrix  $S$ . The scattering matrix can be defined by introducing a set of input and/or output planes or surfaces for the optical element or system and expressing the fields at each surface as a superposition of an appropriate set of orthogonal spatial modes (see Appendix A). The entire set of modes for all the input and output surfaces are labeled sequentially with a single index  $i = 1, 2, \dots, N$ . Each mode can be used to describe a wave propagating toward (input) or away (output) from the optical element. The variables  $a_i(\nu)$  and  $b_i(\nu)$  are used to represent the classical amplitudes of the incoming and outgoing waves for mode  $i$  at frequency  $\nu$ . The definition and normalization of these amplitudes is discussed further in Appendix B; the squares of the wave amplitudes are usually related to energy and power or photon number and rate.

In this paper I only consider linear optical systems for which one would expect to have a linear relationship between the incoming and the outgoing mode amplitudes. This linear relationship defines the scattering matrix:

$$b_i(\nu) = \sum_j S_{ij}(\nu)a_j(\nu). \quad (2)$$

The scattering matrix  $S_{ij}(\nu)$  is a complete characterization of the classical signal properties of the optical element;  $S_{ij}(\nu)$  can also be thought of in quantum mechanical terms as the probability amplitude for a photon that enters the instrument in mode  $j$  to leave the system in mode  $i$ . Although optical engineers might be more familiar with a ray-tracing analysis of optical systems, scattering matrices are indeed sometimes used to design optical elements and systems, especially at long wavelengths.<sup>37–39</sup> Scattering matrices of complex three-dimensional structures can be calculated numerically by use of commercially available electromagnetic simulation software.

Not surprisingly, there is a strong resemblance be-

tween this description of optical systems and the standard scattering matrix formalism for linear circuits used in microwave electronics.<sup>40</sup> In microwave circuit theory, the scattering matrix relates the incoming and outgoing waves that travel on the semi-infinite transmission lines that are attached to the  $N$  ports of a linear network. The scattering matrix  $S_{ij}$  depends on two things: the construction of the circuit in question, and the choice of the characteristic impedance(s) of the transmission lines attached to the circuit. The scattering matrix can easily be converted to the usual electrical quantities such as the impedance or admittance matrices.

An extra term that describes noise can be added to the scattering equation:

$$b_i = \sum_j S_{ij} a_j + c_i. \quad (3)$$

Here  $c_i$  represents the noise wave amplitude radiated by the circuit into transmission line  $i$ . These noise amplitudes are complex Gaussian random variables and are characterized by a Hermitian correlation matrix. For a passive linear circuit in thermal equilibrium at a temperature  $T$ , the noise correlation matrix is given by<sup>35,36,41</sup>

$$\langle c_i c_j^* \rangle = (I - SS^\dagger)_{ij} \frac{h\nu}{2} \coth\left(\frac{h\nu}{2kT}\right) \Delta\nu, \quad (4)$$

where  $\Delta\nu$  is the bandwidth over which the noise is measured. More precisely, we can express the noise cross-spectral density matrix as

$$\begin{aligned} \langle c_i(\nu) c_j^*(\nu') \rangle &= (I - SS^\dagger)_{ij} \frac{h\nu}{2} \coth\left(\frac{h\nu}{2kT}\right) \delta(\nu - \nu') \\ &= C_{ij}^{(\text{class})}(\nu) \delta(\nu - \nu'), \end{aligned} \quad (5)$$

which expresses the fact that noise at different frequencies is uncorrelated. The scattering matrix is unitary for a lossless network,  $SS^\dagger = I$ , since power is conserved, and the noise correlation matrix vanishes as expected. Equation (5) is equivalent to the familiar expression for Johnson–Nyquist voltage noise,

$$\langle \delta V_i(\nu) \delta V_j^*(\nu') \rangle = 2kT(Z + Z^\dagger)_{ij} \delta(\nu - \nu'), \quad (6)$$

in the Rayleigh–Jeans limit  $h\nu \ll kT$ .

## B. Quantum Optics and Quantum Linear Circuits

The quantum mechanical treatment of linear networks or optical systems in terms of input–output operators has been discussed extensively in the quantum optics literature.<sup>5,42–53</sup> In quantum theory, the classical complex wave amplitudes are replaced by operators. In place of Eq. (3) we would write

$$b_i^\dagger(\nu) = \sum_j S_{ij}(\nu) a_j^\dagger(\nu) + c_i^\dagger(\nu), \quad (7)$$

where  $a_i^\dagger(\nu)$  and  $b_i^\dagger(\nu)$  represent photon creation operators that add a photon with frequency  $\nu$  to the incoming or outgoing waves at port (or mode)  $i$ , respectively (see Fig. 1). Yurke and Denker<sup>43</sup> dis-

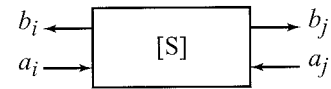


Fig. 1. General linear  $N$ -port network represented by its scattering matrix  $S$ . The incoming waves are represented by complex power amplitudes  $a_i$ , whereas the outgoing waves are represented by  $b_i$ . The scattering matrix relates the outgoing wave amplitudes to the incoming amplitudes. The matrix element  $S_{ij}$  can be considered to be the quantum-mechanical probability amplitude for a photon that enters port  $j$  to emerge at port  $i$ .

cussed the quantization of electrical networks and described how Eq. (7) can be obtained from the Heisenberg equations of motion. The derivation of Eq. (7) for open electromagnetic scattering systems in which the field is not confined to a finite volume has also been discussed.<sup>52,53</sup> In analogy to the situation for classical thermal noise, the noise operators  $c_i^\dagger(\nu)$  are necessary if the network or system has loss. As explained in Appendix B, the quantum scattering matrix  $S_{ij}(\nu)$  used in this equation is exactly the same quantity as would be used to describe the classical network or system.

We expect that the incoming and outgoing photon operators should obey the commutation relations for bosons, namely,

$$[a_i(\nu), a_j^\dagger(\nu')] = \delta_{ij} \delta(\nu - \nu'), \quad (8)$$

$$[b_i(\nu), b_j^\dagger(\nu')] = \delta_{ij} \delta(\nu - \nu'). \quad (9)$$

Commutation relations of this type are standard for describing continuum fields,<sup>53–55</sup> note that the operators have dimensions of (photons/Hz)<sup>1/2</sup>. By using Eq. (7) to express the  $b_i$  and  $b_i^\dagger$  operators in the commutator, we can show that the noise operators must have a commutation relation

$$[c_i(\nu), c_j^\dagger(\nu')] = [I - S(\nu)S^\dagger(\nu)]_{ji} \delta(\nu - \nu'). \quad (10)$$

This result has an interesting similarity to the classical noise correlation matrix [Eq. (5)], as has been noted previously.<sup>44</sup>

Another way to arrive at the same result is to consider any  $N$ -port lossy network as consisting of an extended lossless network with  $N + M$  ports, with scattering matrix  $S'$  (see Fig. 2). The additional  $M$  internal ports are attached to semi-infinite transmission lines that behave as resistors and can therefore account for the losses of the circuit. It is clear physically that such a decomposition should be possible. A good example is a transmission line that has ohmic losses owing to the skin effect in the conductors: we would approximate the transmission line by a discrete ladder network, introducing series resistors to represent the skin effect loss (see Fig. 3). These resistors are then replaced by internal ports that are attached to semi-infinite transmission lines (with appropriate characteristic impedances) to simulate the dissipation of the resistors. The idea of using transmission lines in place of lossy circuit elements dates

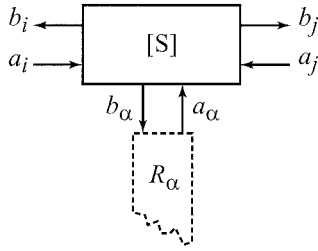


Fig. 2. Any lossy linear  $N$ -port network can be represented by a lossless  $(N + M)$ -port network, in which the extra internal ports, labeled by greek indices  $\alpha = 1, \dots, M$ , are terminated by resistors  $R_\alpha$ . In turn, these resistors can be replaced by semi-infinite transmission lines with characteristic impedances  $R_\alpha$ . In this diagram, the semi-infinite transmission line is represented by the dashed box with one ragged edge.

back to Nyquist,<sup>34</sup> and this construct has seen widespread use in quantum optics calculations.<sup>43,45,46</sup>

Since the extended  $(N + M)$ -port network has no loss, it generates no noise, and we can write

$$b_i^\dagger = \sum_j S_{ij}' a_j^\dagger + \sum_\alpha S_{i\beta}' a_\beta^\dagger, \quad (11)$$

$$b_\alpha^\dagger = \sum_j S_{\alpha j}' a_j^\dagger + \sum_\beta S_{\alpha\beta}' a_\beta^\dagger. \quad (12)$$

Here the roman indices refer to external ports, whereas greek indices are reserved for the internal (resistor) ports. Clearly,  $S_{ij}' = S_{ij}$ . The noise operators for the original circuit are now seen to be related to the photon operators for the incoming waves at the internal ports:

$$c_i^\dagger = \sum_\beta S_{i\beta}' a_\beta^\dagger. \quad (13)$$

From the unitarity of the extended  $(N + M)$ -port scattering matrix  $S'$ , we can show that

$$(I - SS^\dagger)_{ij} = \delta_{ij} - \sum_k S_{ik}' S_{jk}'^* = \sum_\beta S_{i\beta}' S_{j\beta}'^*. \quad (14)$$

This expression, combined with the definition [Eq. (13)] of the noise operators, yields the same noise commutation relations written earlier [Eq. (10)].

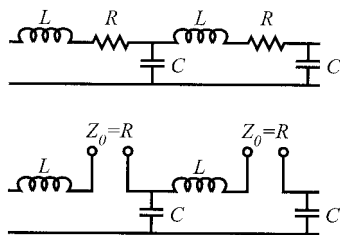


Fig. 3. Top: a discrete ladder approximation to a transmission line, including resistors  $R$  that account for ohmic loss. Bottom: the resistors have been replaced by ports that are attached to semi-infinite transmission lines (not shown) that have characteristic impedance  $Z_0 = R$ .

### C. Thermal Photon Noise Correlation Matrix

We have discussed how Gaussian noise in classical electrical networks can be characterized by a correlation matrix. The same approach can be used for thermal noise in quantum networks. Using Eq. (13), we see that

$$\langle c_i^\dagger(\nu) c_j(\nu') \rangle = \sum_{\alpha, \beta} S_{i\alpha}'(\nu) S_{j\beta}'^*(\nu') \langle a_\alpha^\dagger(\nu) a_\beta(\nu') \rangle. \quad (15)$$

Here the angle brackets represent the quantum statistical average calculated by use of density matrix  $\rho$ :  $\langle A \rangle = \text{Tr}(\rho A)$ . Our basic assumption is that the incoming waves injected into the network from any internal port  $\alpha$  can be considered to be thermal black-body radiation at some temperature  $T_\alpha$ . This is physically reasonable, since the internal ports were introduced to take the place of lossy elements (resistors). The temperature  $T_\alpha$  is just the physical temperature of the lossy element. As shown in Appendix C, our assumption implies that

$$\langle a_\alpha^\dagger(\nu) a_\beta(\nu') \rangle = n_{\text{th}}(\nu, T_\alpha) \delta_{\alpha\beta} \delta(\nu - \nu'), \quad (16)$$

so the correlation of two noise operators takes the form

$$\langle c_i^\dagger(\nu) c_j(\nu') \rangle = C_{ij}(\nu) \delta(\nu - \nu'), \quad (17)$$

where the noise correlation matrix  $C_{ij}(\nu)$  is

$$C_{ij}(\nu) = \sum_\beta S_{i\beta}'(\nu) S_{j\beta}'^*(\nu) n_{\text{th}}(\nu, T_\beta). \quad (18)$$

For the case of an  $N$ -port network, which is in thermal equilibrium at temperature  $T$ , all the temperatures of the internal resistors are equal,  $T_\beta = T$ , so

$$C_{ij}(\nu) = (I - SS^\dagger)_{ij} n_{\text{th}}(\nu, T), \quad (19)$$

which can be derived by use of Eq. (14). Equations (18) and (19) are implicit in other work<sup>50</sup> and are clearly related to the classical noise correlation matrix [Eq. (5)]. In fact, the classical noise correlation matrix corresponds to the symmetrized average

$$\begin{aligned} \frac{h\nu}{2} \langle c_i(\nu) c_j^\dagger(\nu') + c_j^\dagger(\nu') c_i(\nu) \rangle \\ = h\nu (I - SS^\dagger)_{ij} [n_{\text{th}}(\nu, T) + 1/2] \delta(\nu - \nu'), \end{aligned}$$

since  $\coth(h\nu/2kT) = 2n_{\text{th}}(\nu, T) + 1$ . The extra  $h\nu$  factor is necessary because the classical wave amplitudes are normalized to represent power, whereas the quantum operators represent photon creation and destruction.

For a thermal density matrix, the expectation value of a product of an arbitrary number of photon noise operators can be expressed in terms of the two-operator correlation matrix  $C_{ij}(\nu)$  and the scattering matrix  $S_{ij}(\nu)$ . The case of four noise operators is worked out in Appendix C by use of elementary techniques. The general procedure is to apply the commutation relations to move all creation operators to

the left and all destruction operators to the right (to normal order). Having done this, the averages are calculated by summation of all possible pairings of creation and destruction operators; each pair introduces a factor involving  $C_{ij}(\nu)$ . The scattering matrix is needed in addition to  $C_{ij}(\nu)$  because it appears in the expression for the commutator of the noise operators. It is easy to check that this procedure yields Eq. (C9). This result is related to the fact that the average of a product of Gaussian random variables can be expressed in terms of the correlations between pairs of variables; note that use of the coherent state representation<sup>56</sup> to evaluate the operator averages for thermal radiation produces Gaussian integrals.

#### D. Operators for Photon Counting and Bolometric Detectors

A complete detection instrument can be constructed by placement of detectors at the output ports of an optical system. The optical system is characterized in terms of a scattering matrix and a noise correlation matrix; the behavior of a detector can be described by a quantum operator. This operator represents the physical quantity that can be measured with an ideal detector. Real detectors are nonideal and have other sources of noise, such as dark current or amplifier noise, and these additional noise sources must be considered for practical applications.

An ideal photon-counting detector simply measures the number of photons arriving over some integration time  $\tau$  from which the average photon arrival rate can be calculated. For a detector that receives photons only from the  $i$ th port or mode, the appropriate operator for the average arrival rate is

$$d_i = \frac{1}{\tau} \int_0^\tau dt b_i^\dagger(t) b_i(t), \quad (20)$$

where the time-dependent (Heisenberg picture) photon operators are simply the Fourier transforms

$$b_i(t) = \int_0^{+\infty} d\nu \exp(i2\pi\nu t) b_i(\nu), \quad (21)$$

$$b_i^\dagger(t) = \int_0^{+\infty} d\nu \exp(-i2\pi\nu t) b_i^\dagger(\nu). \quad (22)$$

This is a standard representation of an ideal photon detector in the quantum optics literature.<sup>54,55</sup> Although it could appear that we chose to consider only perfect detectors with unit quantum efficiency, in fact we can incorporate detector nonidealities into the linear network that connects the input signal to the detectors. For example, a detector with a 50% quantum efficiency could be simulated by the combination of an attenuator with 50% transmission in front of a perfect detector. Note also that we have chosen to consider only single-mode detectors. The generalization to multimode detectors is straightforward and will be taken up in Section 4. Finally, although the

operator we use for the detector response is simple and appealing, we note that photodetector theory has several subtleties, as discussed in the literature.<sup>57-61</sup>

A bolometric detector measures the average power

$$d_i^{(B)} = \frac{1}{\tau} \int_0^\tau dt b_i^{(B)\dagger}(t) b_i^{(B)}(t), \quad (23)$$

where the time-dependent power amplitude operators are

$$b_i^{(B)}(t) = \int_0^{+\infty} d\nu \exp(i2\pi\nu t) b_i(\nu) \sqrt{h\nu}, \quad (24)$$

$$b_i^{(B)\dagger}(t) = \int_0^{+\infty} d\nu \exp(-i2\pi\nu t) b_i^\dagger(\nu) \sqrt{h\nu}. \quad (25)$$

We concentrate on the case of photon-counting detectors since the expressions for bolometric detectors differ only by factors of  $h\nu$  inside the integrals. For simplicity, from now on we will drop the  $(0, +\infty)$  limits on frequency integrals.

#### E. Statistics of the Detector Outputs: Mean Values

We are now in a position to calculate the mean values of the detector outputs and their fluctuations. First, let us calculate the mean values of the photon output operators:

$$\begin{aligned} \langle b_i^\dagger(\nu) b_j(\nu') \rangle &= \sum_{k,l} S_{ik}(\nu) S_{jl}^*(\nu') \langle a_k^\dagger(\nu) a_l(\nu') \rangle \\ &+ \langle c_i^\dagger(\nu) c_j(\nu') \rangle. \end{aligned} \quad (26)$$

The correlation of the two noise operators is given by Eqs. (17) and (18). However, it is not obvious how to treat the term involving the incoming wave operators,  $\langle a_k^\dagger(\nu) a_l(\nu') \rangle$ . Some of these ports (modes) are inputs to the instrument; others are coupled to the detectors. For best sensitivity, the detectors should be operated at a temperature such that  $kT \ll h\nu$ ; thus  $n_i \approx 0$  when  $i$  is a detector port. Alternatively, the instrument should be designed so that it does not couple the thermal noise emitted by one detector into another detector, i.e.,  $|S_{ij}| = 0$  when  $i$  and  $j$  both correspond to detector ports. However, the input signal could be nonzero and should be coupled into the detectors, so  $n_k \neq 0$  and  $|S_{ik}| \neq 0$  when  $k$  corresponds to an input port and  $i$  is a detector port. One possible choice is to imagine that the inputs are receiving uncorrelated thermal noise, so that

$$\langle a_k^\dagger(\nu) a_l(\nu') \rangle = n_k(\nu) \delta_{kl} \delta(\nu - \nu'). \quad (27)$$

Here  $n_k(\nu)$  are the mean occupation numbers for the incoming modes at the instrument inputs. This is by no means the only possible choice—we can prepare input beams to the instrument in whatever manner we wish, so the answer depends on the experimental situation. The assumption of uncorrelated thermal noise is quite realistic since we are interested primarily in astronomical applications. If we include the telescope and atmosphere in the definition of a

ground-based instrument (a simple method is to treat them as attenuators), the input modes would be defined above the atmosphere, and to a good approximation we could set  $n_i = 0$  since all the dominant thermal noise terms were already included in this definition of the instrument. Noise can either be considered to arise within the instrument or to arrive at an input, depending on how the instrument is defined.

With this understanding, we write

$$\langle b_i^\dagger(\nu)b_j(\nu') \rangle = \delta(\nu - \nu') B_{ij}(\nu), \quad (28)$$

where

$$B_{ij}(\nu) = \sum_k S_{ik}(\nu) S_{jk}^*(\nu) n_k(\nu) + C_{ij}(\nu). \quad (29)$$

The mean value of the output operator for the  $i$ th detector can now be found:

$$\begin{aligned} \langle d_i \rangle &= \frac{1}{\tau} \int_0^\tau dt \langle b_i^\dagger(t) b_i(t) \rangle \\ &= \frac{1}{\tau} \int d\nu d\nu' \int_0^\tau dt \\ &\quad \times \exp[i2\pi(\nu - \nu')t] \langle b_i^\dagger(\nu) b_i(\nu') \rangle \\ &= \int d\nu B_{ii}(\nu). \end{aligned} \quad (30)$$

For bolometric detectors, a factor of  $h\nu$  should be inserted into the integral. The interpretation is clear:  $B_{ii}(\nu)d\nu$  is the mean rate at which photons in the frequency range  $\nu, \nu + d\nu$  are absorbed by the detector; equivalently,  $B_{ii}(\nu)$  is the mean occupancy number of the mode received by the detector.

#### F. Statistics of the Detector Outputs: Covariance Matrix

To discuss the sensitivity of instruments, we must calculate the fluctuations of the detector outputs. These fluctuations are characterized by a covariance matrix

$$\sigma_{ij}^2 = \langle \delta d_i \delta d_j \rangle = \langle d_i d_j \rangle - \langle d_i \rangle \langle d_j \rangle. \quad (31)$$

Thus, we need the quantity

$$\langle d_i d_j \rangle = \frac{1}{\tau^2} \int_0^\tau dt_1 \int_0^\tau dt_2 \langle N_i(t_1) N_j(t_2) \rangle, \quad (32)$$

where  $N_i(t) = b_i^\dagger(t) b_i(t)$ . The average  $\langle N_i(t_1) N_j(t_2) \rangle$  can depend only on the time difference  $\delta t = t_1 - t_2$ . Let us define the symmetrized correlation function

$$\Sigma_{ij}(\delta t) = \langle N_i(t + \delta t) N_j(t) + N_i(t) N_j(t + \delta t) \rangle. \quad (33)$$

Note that  $N_i(t)$  is a Hermitian operator and furthermore it commutes with  $N_j(t')$  for  $i \neq j$ . These facts imply that  $\Sigma_{ij}(\delta t)$  is real, as is the covariance matrix

itself. By changing the integration variables from  $t_1$  and  $t_2$  to  $\delta t$  and  $t_1$ , we find

$$\langle d_i d_j \rangle = \frac{1}{\tau^2} \int_0^\tau d(\delta t) (\tau - \delta t) \Sigma_{ij}(\delta t). \quad (34)$$

Next, we calculate  $\Sigma_{ij}(\delta t)$ , which will require a correlation of four outgoing photon operators. We could calculate this correlation by writing the outgoing photon operators in terms of the incoming photon operators ( $a_i$ ) and noise operators ( $c_i$ ) using Eq. (7), since we have expressions for the fourth-order correlations of these operators [Eqs. (C7) and (C9)]. However, this approach is tedious, and it is easier to apply the general method for working out operator correlations described previously in this Subsection 2.C:

$$\begin{aligned} \Sigma_{ij}(\delta t) &= \int d\nu_1 d\nu_2 d\nu_3 d\nu_4 \langle b_i^\dagger(\nu_1) b_i(\nu_2) b_j^\dagger(\nu_3) b_j(\nu_4) \rangle \\ &\quad \times \{ \exp[-i2\pi(\nu_1 - \nu_2)(t + \delta t)] \\ &\quad \times \exp[-i2\pi(\nu_3 - \nu_4)t] \\ &\quad + \exp[-i2\pi(\nu_1 - \nu_2)t] \\ &\quad \times \exp[-i2\pi(\nu_3 - \nu_4)(t + \delta t)] \} \\ &= \int d\nu_1 d\nu_2 d\nu_3 d\nu_4 [ \langle b_i^\dagger(\nu_1) b_j^\dagger(\nu_3) b_i(\nu_2) b_j(\nu_4) \rangle \\ &\quad + \delta_{ij} \delta(\nu_2 - \nu_3) \langle b_i^\dagger(\nu_1) b_j(\nu_4) \rangle ] \\ &\quad \times \{ \exp[-i2\pi(\nu_1 - \nu_2)(t + \delta t)] \\ &\quad \times \exp[-i2\pi(\nu_3 - \nu_4)t] \\ &\quad + \exp[-i2\pi(\nu_1 - \nu_2)t] \\ &\quad \times \exp[-i2\pi(\nu_3 - \nu_4)(t + \delta t)] \} \\ &= \int d\nu_1 d\nu_2 d\nu_3 d\nu_4 [ B_{ii}(\nu_1) B_{jj}(\nu_3) \delta(\nu_1 - \nu_2) \\ &\quad \times \delta(\nu_3 - \nu_4) \\ &\quad + B_{ji}(\nu_1) (B_{ji}(\nu_3) + \delta_{ij}) \delta(\nu_1 - \nu_4) \delta(\nu_3 - \nu_2) ] \\ &\quad \times \{ \exp[-i2\pi(\nu_1 - \nu_2)(t + \delta t)] \\ &\quad \times \exp[-i2\pi(\nu_3 - \nu_4)t] \\ &\quad + \exp[-i2\pi(\nu_1 - \nu_2)t] \\ &\quad \times \exp[-i2\pi(\nu_3 - \nu_4)(t + \delta t)] \} \\ &= \int d\nu_1 d\nu_3 [ 2B_{ii}(\nu_1) B_{jj}(\nu_3) \\ &\quad + 2B_{ij}(\nu_1) (B_{ji}(\nu_3) + \delta_{ij}) \cos(2\pi(\nu_1 - \nu_3)\delta t) ]. \end{aligned}$$

The first term inserted into Eq. (34) simply yields the product of the averages  $\langle d_i \rangle \langle d_j \rangle$ . The second term yields a time integral of the form

$$2 \int_0^\tau d(\delta t) (\tau - \delta t) \cos[2\pi(\nu_1 - \nu_3)\delta t] \approx \tau \delta(\nu_1 - \nu_3), \quad (35)$$

where the approximation holds for long integration times  $\tau$  such that  $(\nu_1 - \nu_3)\tau \gg 1$ . In other words, if  $\Delta\nu$  is a characteristic spectral resolution of the instrument, we require that the integration time be much longer than the Fourier limit, so  $\tau\Delta\nu \gg 1$ .

Thus, the covariance matrix of the detector outputs is simply

$$\sigma_{ij}^2 = \frac{1}{\tau} \int d\nu B_{ij}(\nu)(B_{ji}(\nu) + \delta_{ij}). \quad (36)$$

For bolometric detectors, a factor of  $(h\nu)^2$  should be inserted into the integral. Equation (36) and Eqs. (26) and (29) are the key results of this paper.

Note that  $B_{ii}(\nu)$  is real and  $B_{ij}(\nu) = B_{ji}^*(\nu)$ , so the covariance matrix  $\sigma_{ij}^2$  is real, as promised. To calculate the fluctuations of the  $i$ th detector, we see that it is only necessary to know the diagonal term  $B_{ii}(\nu)$ , which is just the mean photon occupancy of the mode received by the detector. However, to calculate the correlation of the noise at two different detectors, it is necessary to know the off-diagonal terms  $B_{ij}(\nu)$  as well. An important aspect of this result can already be seen. If the background incident on all the detectors is low (low occupancy number), i.e.,  $B_{ii}(\nu) \ll 1$  for all  $i$ , then the fluctuations are not highly correlated: for  $i \neq j$ ,  $\sigma_{ij}^2 \ll \sigma_{ii}^2$  and  $\sigma_{ij}^2 \ll \sigma_{jj}^2$ . These follow immediately from the inequality  $|B_{ij}(\nu)|^2 \leq B_{ii}(\nu)B_{jj}(\nu)$ , which itself is not difficult to demonstrate.

### G. Quantum Network Calculations

Any passive linear network with thermal noise sources can be completely characterized by its scattering matrix  $S_{ij}(\nu)$  and its noise operator correlation matrix  $C_{ij}(\nu)$ . Do general algorithms exist to calculate these matrices for instruments of arbitrary complexity? It is clear that this problem is quite closely related to classical microwave circuit theory. In fact, the calculation of the scattering matrix is exactly the same for both cases and can be done by use of a variety of techniques, including, for example, the wave methods discussed by Wedge and Rutledge.<sup>41,62–64</sup> These methods allow one to start out with simple elements whose scattering matrices are known and to build up complicated networks by making connections between the elements. These techniques have been extended to compute the classical noise correlation matrix as well.<sup>63</sup> It is easy to convert the classical noise correlation matrix of a passive circuit, calculated with Eq. (5) for each circuit element, into the corresponding quantum noise operator correlation matrix:

$$C_{ij}^{(\text{quant})}(\nu) = \frac{1}{h\nu} C_{ij}^{(\text{class})}(\nu) - \frac{1}{2} (I - SS^\dagger)_{ij}, \quad (37)$$

which again is a result of  $\coth(h\nu/2kT) = 2n_{\text{th}}(\nu, T) + 1$ . Thus, in principle we can use standard microwave circuit programs or algorithms to evaluate the quantum scattering matrix and quantum noise correlation matrix of any passive linear network or op-

tical system from the scattering and noise matrices of the individual components. It is important, however, that the microwave program use the full Callen–Welton formula,  $h\nu \coth(h\nu/2kT)/2$ , and not just the Rayleigh–Jeans approximation  $kT$ . Alternatively, if the source code is available, the microwave circuit program could be modified to evaluate noise correlation matrices by use of Eq. (19) instead of Eq. (5). Such a program is readily available.<sup>65,66</sup>

An interesting application of these techniques is the quantum optics of dielectric materials that are dispersive and lossy. This is a topic that has been treated fairly recently in the literature,<sup>47,48</sup> by use of methods in which the electromagnetic field in the dielectric material is quantized. The circuit concepts and algorithms discussed above could easily be applied to such problems. For example, a specific problem that has been analyzed in detail is a multilayer stack of uniform dielectric slabs. It is well known that translational symmetry can be used to reduce this problem to a set of equivalent transmission lines connected in cascade. One could use this equivalence to calculate the scattering matrix of each slab, and the quantum noise operator correlation matrix for the slab could then be calculated by use of Eq. (19). Using the connection algorithms for microwave circuits, one could combine these matrices for the individual slabs to determine the overall scattering and noise operator correlation matrices for the entire stack. If the multilayer stack is isothermal, the noise correlation matrix could be directly calculated from the scattering matrix.

## 3. Results for Single-Mode Detectors

### A. Instruments with a Single Input

To gain confidence in the results, we examine a few simple cases. We analyze an instrument that has one single-mode input, which we label as the  $i = 0$  port, and one or more output ports  $i = 1, \dots, N$  that feed detectors. Examples of such instruments include a single-beam photometer and a single-beam spectrometer with multiple spectral channels (e.g., a grating spectrometer). We assume that the detectors are cold ( $kT \ll h\nu$ ) and do not inject thermal noise into the system; thus  $n_i = 0$  for  $i \neq 0$ . The input signal can be nonzero and should be coupled to the detectors:  $n_0 \neq 0$  and  $|S_{i0}(\nu)| \neq 0$  in general. Under these assumptions, Eq. (29) indicates that

$$B_{ij}(\nu) = S_{i0}(\nu)S_{j0}^*(\nu)n_0(\nu) + C_{ij}(\nu), \quad (38)$$

and the mean detector output from Eq. (30) is

$$\langle d_i \rangle = \int d\nu [ |S_{i0}(\nu)|^2 n_0(\nu) + C_{ii}(\nu) ]. \quad (39)$$

From the first term in this expression, it is obvious that a photon with frequency  $\nu$  that enters the instrument has a probability  $|S_{i0}(\nu)|^2$  to be absorbed in the  $i$ th detector. The second term gives us the rate of dark counts due to photons generated thermally in-

side the instrument. The covariance matrix of the detector outputs is obtained from Eq. (36):

$$\begin{aligned} \sigma_{ij}^2 = & \frac{1}{\tau} \int d\nu |S_{i0}(\nu)|^2 n_0(\nu) [|S_{j0}(\nu)|^2 n_0(\nu) + \delta_{ij}] \\ & + C_{ij}(\nu) [C_{ji}(\nu) + \delta_{ij}] \\ & + 2 \operatorname{Re}[S_{i0}^*(\nu) S_{j0}(\nu) C_{ij}(\nu)] n_0(\nu). \end{aligned} \quad (40)$$

### B. Noise-Equivalent Power of a Single-Channel System

For a single detector at the output of a lossless or cooled filter that does not generate noise, so that  $C_{ij}(\nu) = 0$ , Eq. (40) gives the variance of the detector output:

$$\sigma^2 = \frac{1}{\tau} \int d\nu \eta(\nu) n_0(\nu) [\eta(\nu) n_0(\nu) + 1]. \quad (41)$$

Here  $\eta(\nu) = |S_{i0}(\nu)|^2$  is the power (or photon) transmission of the filter. We see that this expression is identical to the standard expression for the noise in a single-mode detector with quantum efficiency  $\eta(\nu)$ .<sup>13,16–19,26</sup> In particular, the quantum efficiency correctly multiplies the bunching term.

This result can be converted into an expression for the noise-equivalent power. The mean detector output is

$$\langle d \rangle = \int d\nu \eta(\nu) n_0(\nu). \quad (42)$$

For a narrowband filter,  $\Delta\nu \ll \nu$ , we can approximate the integrals

$$\langle d \rangle = \eta n_0 \Delta\nu \quad (43)$$

$$\sigma^2 = \frac{1}{\tau} \eta n_0 (1 + \eta n_0) \Delta\nu. \quad (44)$$

The power that enters the input port is  $P = h\nu n_0 \Delta\nu = h\nu \langle d \rangle / \eta$ . The uncertainty in the input power after an integration time  $\tau$  for a background-limited detector is given by

$$\sigma_P = \frac{h\nu\sigma}{\eta} = \frac{h\nu}{\sqrt{\Delta\nu\tau}} \sqrt{\frac{n_0(1 + \eta n_0)}{\eta}} \Delta\nu, \quad (45)$$

which when calculated for an integration time  $\tau = 0.5$  s (corresponding to a postdetection bandwidth of 1 Hz) gives the noise-equivalent power. This is the result given in Eq. (1).

To verify Eq. (45), we work out the limiting forms for high and low background levels. In the radio case,  $n_0 \approx kT_0/h\nu \gg 1$ , where  $T_0$  is the equivalent Rayleigh–Jeans temperature of the background radiation and

$$\sigma_P \approx \frac{kT_0}{\sqrt{\Delta\nu\tau}} \Delta\nu, \quad (46)$$

which is just the standard Dicke equation for the sensitivity of a radiometer. In the optical case,  $n_0 \ll 1$ , and

$$\sigma_P \approx \frac{h\nu}{\eta\tau} \sqrt{\eta n_0 \Delta\nu\tau}. \quad (47)$$

The quantity inside the square root is simply the number of photons counted by the detector in time  $\tau$ . The prefactor converts this Poisson uncertainty in the photons counted into a power uncertainty at the input of the system. Thus, we recover the well-known results for the background-limited sensitivity of a single detector in both regimes. Note that both terms under the square root in Eq. (45) are needed to reproduce the two limiting cases.

### C. Detector Preceded by a Quantum-Limited Amplifier

We can also investigate the sensitivity of a detector that is preceded by a high-gain linear amplifier. In this case, we expect to find that the minimum possible noise is set by the standard quantum limit for phase-insensitive amplifiers.<sup>5</sup> Amplifier noise can be treated simply by letting  $T \rightarrow 0^-$  in the thermal noise formulas; physically, negative excitation temperatures correspond to inverted level populations in maser or laser amplifiers.<sup>42,46</sup> In the  $T \rightarrow 0^-$  limit, the noise correlation matrix can easily be shown to be

$$C_{ij}(\nu) = (SS^\dagger - I)_{ij}. \quad (48)$$

Applying this to a two-port amplifier with perfect input match, output match, and reverse isolation ( $|S_{11}| = |S_{22}| = |S_{12}| = 0$ ), and power gain  $G(\nu) = |S_{21}(\nu)|^2$  yields  $C_{22}(\nu) = G(\nu) - 1$ . Here we follow the microwave engineering convention: port 1 is the amplifier input and port 2 is the output. If the input to the amplifier is thermal noise characterized by an occupation number  $n(\nu)$ , we see that the fluctuations of a photon detector connected to the amplifier output are given by

$$\begin{aligned} \sigma_{22}^2 = & \frac{1}{\tau} \int d\nu B_{22}(\nu) [B_{22}(\nu) + 1] \\ = & \frac{1}{\tau} \int d\nu G^2(\nu) [n(\nu) + 1 - G^{-1}(\nu)] [n(\nu) + 1]. \end{aligned}$$

Assuming  $G \gg 1$  and converting the output fluctuations to an uncertainty in the input power, we find

$$\sigma_P = \sqrt{\frac{\Delta\nu}{\tau}} h\nu [n(\nu) + 1]. \quad (49)$$

Note that this expression includes both the amplifier noise as well as the fluctuations of the background radiation. The amplifier contribution can be isolated by setting  $n(\nu) = 0$ . If we express the amplifier noise in terms of an equivalent noise temperature by using the Dicke equation [approximation (46)], we find  $T_n = h\nu/k_B$ , which is the standard quantum limit. If we now imagine that we attach a cold attenuator with transmission  $\eta$  to the amplifier input,

we find that the equivalent noise referred to the attenuator input is given by

$$\sigma_P = \sqrt{\frac{\Delta\nu}{\tau}} \frac{h\nu}{\eta} [\eta n(\nu) + 1], \quad (50)$$

where  $n(\nu)$  now represents the occupation number of the noise that enters the attenuator input. In this case the minimum noise temperature is  $T_n = h\nu/\eta k_B$ . This limit also applies for heterodyne receivers constructed by use of detectors with quantum efficiency  $\eta < 1$ . The sensitivities of direct detection and coherent detection can be compared by use of Eqs. (45) and (50); the sensitivities are equal if  $n \gg 1$ .

#### 4. Multimode Detectors

##### A. Introduction

We begin by outlining some of the difficulties associated with the expressions that appear in the literature for the background-limited sensitivity of multimode detectors. The standard result<sup>18,19</sup> for the  $1\sigma$  uncertainty in the average power absorbed in a bolometric detector during an integration time  $\tau$  is

$$\sigma^2 = \frac{1}{\tau} \left[ \int_0^\infty d\nu h\nu \eta(\nu) P(\nu) + \int_0^\infty d\nu \frac{\eta^2(\nu) P^2(\nu)}{N(\nu)} \right], \quad (51)$$

where  $\eta(\nu)$  is the quantum efficiency,  $P(\nu)d\nu$  is the thermal radiation power incident on the detector in a bandwidth  $d\nu$  centered at frequency  $\nu$ , and  $N(\nu) = 2A\Omega/\lambda^2$  is the effective number of spatial and polarization modes received by a polarization-insensitive detector ( $A$  is the detector area and  $\Omega$  is the solid angle of the illumination). Note that to convert  $\sigma$  to an uncertainty in the incident power one must divide by the quantum efficiency. Richards<sup>19</sup> has raised the issue of whether there is significant theoretical or experimental justification for the second term of Eq. (51). However, as discussed in Section 3, the second term is needed to recover the Dicke radiometer equation for single-mode detectors in the high background limit. Thus, overwhelming theoretical and empirical support exists for the limiting value of the second term when  $N(\nu) \rightarrow 1$ . The only remaining issue is whether the variation of the second term with the number of modes  $N(\nu)$  is given correctly by Eq. (51).

As Lamarre<sup>18</sup> correctly points out, Eq. (51) assumes that all the  $N(\nu)$  radiation modes landing on the detector are equally illuminated and must be modified if this is not the case. To see this, let us examine the single-mode case ( $N = 1$ ). We can express the incident power in terms of the mean occupation number  $P(\nu) = n(\nu)h\nu$ , and so Eq. (51) reads

$$\sigma^2 = \frac{1}{\tau} \int_0^\infty d\nu (h\nu)^2 \eta(\nu) n(\nu) [1 + \eta(\nu) n(\nu)]. \quad (52)$$

This is simply the single-mode result we derived previously [Eq. (41)] with the factor  $(h\nu)^2$  inserted for a

bolometric detector. If instead we detect multiple modes with occupation numbers  $n_i(\nu)$ , we would instinctively try to treat them as being statistically independent and sum their variances. This would indeed reproduce the first term of Eq. (51), since  $P(\nu) = h\nu \sum_i n_i(\nu)$ ; however, for the second term we would obtain  $\sum_i n_i^2(\nu)$  instead of  $P^2(\nu)/N \propto [\sum_i n_i(\nu)]^2/N$ . There is no discrepancy if all the mode occupation numbers are equal, since both sums give  $Nn^2(\nu)$  in that case. However, if only one mode is illuminated, Eq. (51) will clearly underestimate the noise, since it gives a result less than Eq. (52). We should not expect that increasing the number of modes received by a detector could actually cause the fluctuations in the total received power to decrease. This argument shows that Eq. (51) cannot be entirely correct: it fails when the  $N(\nu)$  modes are not equally illuminated.

However, simply summing the variances for the various modes according to Eq. (52) also cannot be correct. Here the difficulty is that the result could depend on the choice of the modes we use to describe the radiation, and this dependence cannot be physical. We can imagine starting with some set  $A$  of (orthogonal) modal functions describing the incoming radiation and illuminating only the first mode, so that  $n_i^A = 0$  for  $i \neq 1$ . We could now change into a new basis  $B$  to describe the modes, and if suitably chosen, all the modes in the new basis can have equal illumination:  $n_i^B = n_1^A/N$ . Clearly  $\sum_i n_i^2$  will be different for these two cases, leading to different calculated sensitivities even though the physical situation has not changed.

What we are failing to consider when we simply sum the mode variances according to Eq. (52) is the possibility that the noise in the various modes could be correlated. In turn, the photon noise and the correlations between modes depends on how the modes are illuminated. This was recognized by Lamarre,<sup>18</sup> who worked out the noise in multimode detectors by use of the semiclassical detection theory of Hanbury Brown and Twiss<sup>26</sup> and the coherence theory of classical optics. For several physical situations, Lamarre calculated the effective number of modes [ $1/\Delta(\nu)$  in his notation], which replaces  $N(\nu)$  in the sensitivity equation [Eq. (51)]. Note that illumination of the modes is not determined purely by the design of the instrument, but can also depend on the source that the instrument is viewing. For example, if an imaging array is used to observe a bright localized source, the photon noise due to the source could overwhelm the background noise (e.g., from the telescope or atmosphere) for the pixels located on or near the image of the source. For these pixels, the effective number of illuminated modes is more strongly related to the coupling of the detector to the source rather than the coupling of the detector to the background radiation. Furthermore, the photon noise at different pixels could be correlated if the temperature of the source is large enough so that  $kT > h\nu$ . In Subsection 4.B, we present a general analysis of the multimode detector problem.

## B. Sensitivity of Multimode Detectors

The photon noise in the case of a multimode detector can easily be treated by use of our results. If a detector is sensitive to more than one mode of the radiation field, one can obtain the average photon arrival rate at the detector by summing over the modes  $o$  that the detector is sensitive to:

$$\langle d \rangle = \sum_o \eta_o \langle d_o \rangle. \quad (53)$$

These modes could be Gauss–Hermite modes or multipole modes expressed by use of vector spherical harmonics; any orthogonal basis can be used. The quantum efficiency factors  $\eta_o$  describe how well a particular mode  $o$  is received by the detector.

The input to the optical system that feeds the detector(s) can also be expanded in a set of modes. Let  $M_I$  represent the set of input modes and  $M_O$  the set of output modes. The multimode optical system that couples the input modes to the output modes can be represented by a scattering matrix. The matrix elements  $S_{oi}(\nu)$  with  $o \in M_O$ ,  $i \in M_I$  describe how light propagates from the input modes to the output modes (received by the detector). Clearly, the effects of the modal quantum efficiency factors  $\eta_o$  can be included in the definition of the scattering matrix; in this case, we would write the mean detector output as

$$\langle d \rangle = \sum_o \langle d_o \rangle. \quad (54)$$

The multimode scattering matrix is often useful when calculating the properties of an optical component or system.<sup>37</sup> In some cases, to a good approximation a simple one-to-one correspondence can be made between the input and the output modes, such that there is no transfer of photons between modes and each mode maintains its identity as it propagates through the system. In other cases, this is not possible; for example, there can be mode conversion due to truncation at finite-sized apertures in a system. In general, a multimode optical system with internal losses will also generate thermal noise that can be characterized by a set of noise operators and their correlation matrix  $C_{ij}(\nu)$ .

If the scattering and noise correlation matrices of a multimode optical system are known, we can determine the photon noise in the detector. As before, we make the simplifying assumption that the detector is cold enough so that it does not emit any significant amount of thermal noise into the optical system. The variance of the detector output is

$$\begin{aligned} \sigma^2 &= \sum_{o,p} \langle \delta d_o \delta d_p \rangle, \text{ where } o, p \in M_O \\ &= \sum_{o,p} \sigma_{op}^2, \end{aligned}$$

and, using Eq. (36), we obtain our general result for multimode detectors:

$$\sigma^2 = \sum_{o,p \in M_O} \frac{1}{\tau} \int d\nu B_{op}(\nu) [B_{po}(\nu) + \delta_{op}]. \quad (55)$$

To check Eq. (55), we can try a few limiting cases. First, consider a system in which the  $N$  input modes each are illuminated with uncorrelated thermal noise with mean occupancy  $n(\nu)$ , and each mode propagates independently (no mode conversion) through a cold instrument (no added noise) with the same transmission probability  $\eta(\nu)$  for each mode. From Eq. (29) we have

$$B_{op}(\nu) = \eta(\nu)n(\nu)\delta_{op}, \quad (56)$$

so

$$\sigma^2 = N \frac{1}{\tau} \int d\nu \eta(\nu)n(\nu)[1 + \eta(\nu)n(\nu)], \quad (57)$$

which agrees with the standard result [Eq. (51)], apart from the usual  $(h\nu)^2$  factor for bolometric detectors.

Another interesting limiting case occurs when only one input mode  $i$  is illuminated, but the input mode has nonzero scattering amplitudes  $|S_{oi}|$  to reach the detector in  $N$  different modes  $o \in M_O$ . In this situation,

$$B_{op}(\nu) = S_{oi}(\nu)S_{pi}^*(\nu)n(\nu). \quad (58)$$

Note that this implies that the modes that arrive at the detector are (fully) correlated. Using Eq. (55) yields

$$\begin{aligned} \sigma^2 &= \frac{1}{\tau} \int d\nu \sum_o |S_{oi}(\nu)|^2 n(\nu) \left[ 1 + \sum_p |S_{pi}(\nu)|^2 n(\nu) \right] \\ &= \frac{1}{\tau} \int d\nu \eta(\nu)n(\nu)[1 + \eta(\nu)n(\nu)], \end{aligned} \quad (59)$$

where  $\eta(\nu) = \sum_o |S_{oi}(\nu)|^2$  is the total probability (quantum efficiency) for an input photon to reach the detector. We see that the photon noise corresponds to the case of a single-mode detector, which is what we expected since only one input mode was illuminated.

## 5. Spectrometer Sensitivity

### A. Overview

The Hanbury Brown and Twiss noise correlations among detectors can play a key role in determining instrument performance. Autocorrelation spectrometers provide a good example. Such spectrometers are commonly used for radio astronomy but not at optical wavelengths. In principle, a direct-detection autocorrelation spectrometer could be built for optical wavelengths. However, we will see that its sensitivity would be inferior to a standard grating spectrometer for low photon occupation numbers, in which case the photon noise at the detector outputs is

uncorrelated. At high occupation numbers, the output noise becomes strongly correlated, which allows the sensitivity of the autocorrelation spectrometer to become competitive.

## B. Spectrometer Types

A nearly ideal optical spectrometer can be produced by combining an efficient diffraction grating with a linear detector array. The photons in the input beam are sorted according to wavelength by the grating and are absorbed by the detector array. The photon counts in the detectors give the spectrum directly, and the noise in the spectrum is, in principle, limited only by the Poisson statistics of photon counting. The closest radio analog of an optical grating spectrometer is a filter bank, in which a large number of filters with contiguous passbands are used to measure the power spectrum.<sup>67</sup> The signal that the filter bank processes has already been amplified by a front-end receiver; but this is only a technical detail, since in most cases the thermal backgrounds are large,  $n \gg 1$ , and an amplifier need not add a significant amount of noise.

Filter banks have largely fallen out of favor and have often been replaced by correlation spectrometers because they are usually easier to build.<sup>68–70</sup> Correlators use the fact that the autocorrelation function of the receiver output voltage waveform  $V(t)$ , defined as

$$A(\delta t) = \langle V(t)V(t - \delta t) \rangle = A(-\delta t), \quad (60)$$

is the Fourier transform of the power spectrum  $S(\nu)$  of the receiver output

$$\begin{aligned} A(\delta t) &= \int_{-\infty}^{+\infty} d\nu \exp(i2\pi\nu\delta t)S(\nu) \\ &= 2 \int_0^{+\infty} d\nu \cos(2\pi\nu\delta t)S(\nu), \end{aligned} \quad (61)$$

and vice versa,

$$S(\nu) = 2 \int_0^{+\infty} d(\delta t) \cos(2\pi\nu\delta t)A(\delta t). \quad (62)$$

A correlation spectrometer directly measures the function  $A(\delta t_l)$  for a discrete set of delays or lags  $\{\delta t_1, \delta t_2, \dots, \delta t_{N_{\text{lags}}}\}$ . Typically, transmission lines or digital shift registers are used to generate the delays, transistor voltage multipliers or digital circuits perform the multiplication, and low-pass filters or digital counters perform the time averaging. It is well known (at least by radio astronomers) that correlation and filter bank spectrometers have equivalent sensitivities for classical signals.

A natural question arises: can correlation techniques be used for optical spectroscopy? How would the sensitivity compare with a grating spectrometer? In the radio case, amplifiers can be used to make extra copies of the signal  $V(t)$  to feed the multiple

delays, without adding any significant amount of noise. However, in the optical case, the noise penalty associated even with an ideal quantum-limited amplifier is too large, so the input beam must somehow be split to feed the delays, and therefore any individual delay would receive only a fraction of the photons in the input beam. Does this imply a loss of sensitivity? If so, is the photon occupation number in the input beam the crucial quantity to consider, or is it the occupation number of the mode arriving at some detector? These issues are addressed below.

## C. Response of Single-Mode Spectrometers

A single-mode spectrometer has a single input port or mode, which we label with the index  $i = 0$ , and  $N_{\text{det}}$  output ports or modes that feed detectors, labeled  $i = 1, \dots, N_{\text{det}}$ . For simplicity we assume that the spectrometer is lossless or cold and adds no noise. According to Eq. (39), the photon counts  $D_i$  in the detectors have average values  $\mu_i = \langle D_i \rangle = \langle d_i \rangle \tau$  given by

$$\mu_i = \tau \int d\nu |S_{i0}(\nu)|^2 n_0(\nu). \quad (63)$$

From Eq. (40), the covariance matrix of the photon count fluctuations  $\delta D_i = D_i - \mu_i$  is

$$\begin{aligned} C_{ij}^{(D)} &= \langle \delta D_i \delta D_j \rangle \\ &= \tau \int d\nu |S_{i0}(\nu)|^2 n_0(\nu) [|S_{j0}(\nu)|^2 n_0(\nu) + \delta_{ij}]. \end{aligned} \quad (64)$$

To make progress, we must restrict the form of the input spectrum  $n_0(\nu)$  so that it can be parameterized by  $N_{\text{chan}}$  quantities that can, in principle, be estimated from the  $N_{\text{det}}$  detector counts. Clearly, we must require  $N_{\text{chan}} \leq N_{\text{det}}$ . We choose a simple histogram or channel spectrum of the form

$$n_0(\nu) = \sum_{c=1}^{N_{\text{chan}}} \bar{n}_c U_c(\nu), \quad (65)$$

where the indicator function  $U_c(\nu)$  is unity for frequencies within the spectral channel  $c$ ,  $\nu_c \leq \nu \leq \nu_{c+1}$ , which has width  $\Delta\nu_c = \nu_{c+1} - \nu_c$ , and is zero otherwise. We define  $P$ , the photon detection probability matrix,<sup>7</sup> by its elements

$$p_{ic} = \frac{1}{\Delta\nu_c} \int_{\nu_c}^{\nu_{c+1}} d\nu |S_{i0}(\nu)|^2. \quad (66)$$

It can readily be shown that  $0 \leq p_{ic} \leq 1$  and  $\sum_i p_{ic} \leq 1$ . The mean number of input photons in channel  $c$  during an integration time  $\tau$  is defined as

$$\lambda_c = \bar{n}_c \Delta\nu_c \tau. \quad (67)$$

With these definitions, we can rewrite the mean photon counts [Eq. (63)] as

$$\mu_i = \sum_c p_{ic} \lambda_c, \quad (68)$$

and the covariance matrix [Eq. (64)] as

$$C_{ij}^{(D)} = \mu_i \delta_{ij} + \sum_c p_{ic} p_{jc} \rho_{ijc} \lambda_c \bar{n}_c, \quad (69)$$

where we have introduced

$$\rho_{ijc} = \frac{1}{p_{ic} p_{jc} \Delta v_c} \int_{v_c}^{v_{c+1}} dv |S_{i0}(v)|^2 |S_{j0}(v)|^2. \quad (70)$$

If the response functions  $|S_{i0}(v)|^2$  are nearly constant over the width of a spectral channel, then  $\rho_{ijc} \approx 1$ .

#### D. Spectrometer Sensitivity for Low Occupation Number

For low occupation numbers,  $\bar{n}_c \ll 1$ , we can ignore the second term in Eq. (69) that is due to bunching. In this case the detector outputs are uncorrelated since the correlation matrix is diagonal,  $C^{(D)} = \text{diag}(\mu_1, \mu_2, \dots)$ , as expected from independent Poisson statistics. This problem has been analyzed in detail, and sensitivity limits have been derived by use of the Cramér–Rao theorem.<sup>7</sup> This analysis shows that the only way to obtain optimum sensitivity is to use an ideal instrument, whose photon detection probability matrix is the identity matrix  $p_{ic} = \delta_{ic}$  or  $P = I$ . In other words, the instrument must sort photons by spectral channel prior to detection, which is exactly what a grating spectrometer does. For this case, the raw detector counts provide the estimated spectrum,  $\hat{\lambda}_c = D_c$ , and so the spectral channels are uncorrelated and have fluctuations of  $\sqrt{\lambda_c}$ :

$$C_{ij}^{(\hat{\lambda})} = \text{diag}(\lambda_1, \lambda_2, \dots), \quad (71)$$

which is indeed the best that can be done.

Correlation spectrometers do not satisfy the condition  $P = I$ , and so cannot achieve the optimum sensitivity. What is their sensitivity in the low- $n$  limit? To answer this question, we must adopt a procedure for estimating the spectrum from the detector counts. A simple method for the case  $N_{\text{chan}} = N_{\text{det}}$  (so  $P$  is a square matrix) is to invert  $P$ :

$$\hat{\lambda} = P^{-1}D. \quad (72)$$

Here  $D$  is the vector of detector counts, and  $\hat{\lambda}$  is a vector whose components  $\hat{\lambda}_c$  give the estimated spectrum. In fact, this is the maximum-likelihood estimator,<sup>7</sup> and actually achieves the Cramér–Rao sensitivity bound. Also, this estimator is unbiased, as can be verified by use of Eq. (68). In the more general case, when  $N_{\text{chan}} < N_{\text{det}}$ , we can still use an unbiased linear method:

$$\hat{\lambda} = (P^T P)^{-1} P^T D, \quad (73)$$

which is often called the least-squares estimator.<sup>7</sup> This estimator can also achieve the Cramér–Rao bound when the mean detector counts are all equal, which is often at least approximately true. The covariance matrix of the estimated spectrum can now be calculated:

$$C_{ij}^{(\hat{\lambda})} = \langle \delta \hat{\lambda}_i \delta \hat{\lambda}_j^T \rangle = A C^{(D)} A^T, \quad (74)$$

where  $A$  is the inversion matrix,

$$A = (P^T P)^{-1} P^T. \quad (75)$$

Note that  $A = P^{-1}$  when  $P$  is square.

#### E. Spectrometer Sensitivity for High Occupation Number

For high photon occupation numbers,  $\bar{n}_c \gg 1$ , the second term of Eq. (69) dominates, and so the detector outputs are now correlated. The expression for the covariance matrix can be written for the simplified case that  $\rho_{ijc} = 1$ , which occurs when the response functions are essentially constant across the spectral channels  $\Delta v_c$ . In this case we see that

$$C_{ij}^{(D)} = \sum_c p_{ic} p_{jc} \frac{\lambda_c^2}{\Delta v_c \tau}. \quad (76)$$

We can understand this result in a simple way. First, we rewrite the response equation [Eq. (68)] in terms of the actual photon counts rather than their mean:

$$D_i = \sum_c p_{ic} N_c. \quad (77)$$

Here  $N_c$  represents the actual number of incident photons in spectral channel  $c$ . We expect  $N_c$  to have a mean value  $\langle N_c \rangle = \lambda_c$  and to have uncorrelated channel fluctuations that follow the Dicke radiometer equation:

$$C_{cc'}^{(N)} = \langle \delta N_c \delta N_{c'} \rangle = \frac{\lambda_c^2}{\Delta v_c \tau} \delta_{cc'}. \quad (78)$$

Combining Eqs. (77) and (78) yields Eq. (76). The factors  $\rho_{ijc}$  (which we have set to unity) can be thought of as bandwidth corrections to account for the shape of the spectral response of the various spectrometer outputs.

What is the noise in the resulting spectrum? For the simple linear inversion procedure given in Eq. (73), the covariance matrix of the estimated spectrum is still given by Eq. (74). However, we can write Eq. (76) in matrix form as

$$C^{(D)} = P C^{(N)} P^T, \quad (79)$$

which yields

$$C_{ij}^{(\hat{\lambda})} = C^{(N)} = \text{diag} \left( \frac{\lambda_1^2}{\Delta v_1 \tau}, \frac{\lambda_2^2}{\Delta v_2 \tau}, \dots \right), \quad (80)$$

so the noise in the estimated spectrum is uncorrelated and is given by the Dicke radiometer equation, which is the best that can be done. This result holds regardless of the form of the probability matrix  $P$ , in contrast with the situation at low occupation number. In particular, it is not even necessary for the spectrometer to have high transmission (high quantum efficiency). Note, however, that we had to assume that  $\rho_{ijc} \approx 1$ ; this can be interpreted to mean that the spectrometer must actually detect the full input bandwidth to achieve the Dicke sensitivity.

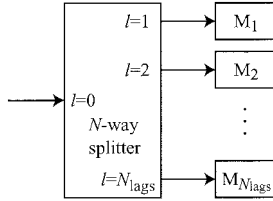


Fig. 4. Schematic diagram of a direct-detection correlation spectrometer. The input signal is first split  $N_{\text{lags}}$  ways; the power transmission is assumed to be  $1/N_{\text{lags}}$ . Each of the splitter outputs is then fed to a Mach-Zehnder interferometer (see Fig. 5), represented by the boxes labeled  $M_l$ , which incorporate the necessary delays and detectors to produce the lag outputs. Interferometer  $M_l$  is set with a fixed time delay (or path-length difference) equal to  $\delta t_l$ .

#### F. Numerical Example: a Direct-Detection Autocorrelator

In this section, I present the results of numerical calculations of the sensitivity of a direct-detection correlator. A possible architecture for such a correlator is shown in Figs. 4 and 5. The idea is simple: the incoming light is split into  $N_{\text{lags}}$  beams, and each beam is analyzed with an interferometer with a fixed time delay (path-length difference)  $\delta t_l$ . The interferometer shown in Fig. 5 is a Mach-Zehnder and allows the use of two detectors that together absorb all the incoming photons. Alternatively, one output port of the Mach-Zehnder interferometer can be terminated, leaving one detector per lag. This architecture could be implemented by use of free-space beam propagation or by use of guided-wave techniques as shown in the figures.

We assume that the delays are evenly spaced:  $\delta t_l = l\Delta t$  for  $l = 0, 1, \dots, N_{\text{lags}} - 1$ . The bandwidth of the correlator is limited by the Nyquist condition,  $\nu_{\text{max}} = 1/(2\Delta t)$ . It is easiest to choose units in which  $\Delta t = 1$ . Like a grating, this type of spectrometer could be operated in higher order, which might be advantageous if only a small fractional bandwidth needs to be analyzed or if the fractional bandwidth of the components is limited.

The sensitivity calculation is straightforward. We label the detectors with our standard indices,  $1 \leq i, j \leq N_{\text{det}}$ . When we use two detectors per lag, we have  $N_{\text{det}} = 2N_{\text{lags}}$ ; otherwise  $N_{\text{det}} = N_{\text{lags}}$ . For the

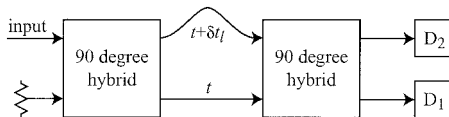


Fig. 5. Mach-Zehnder interferometer made with  $90^\circ$  hybrids that are equivalent to 50% beam splitters. The path-length difference between the two arms is  $\delta t_l$ . The drawing shows detectors for both outputs of the interferometer ( $D_1$  and  $D_2$ ). It is possible to use just one detector per lag; to do this,  $D_2$  should be replaced by a termination (a perfect absorber). The power transmission from the input to  $D_1$  is  $\cos^2(\pi\nu\delta t_l)$ , and the transmission from the input to  $D_2$  is  $\sin^2(\pi\nu\delta t_l)$ . With both detectors present, the total quantum efficiency is unity; with only one detector, the average quantum efficiency is 50%.

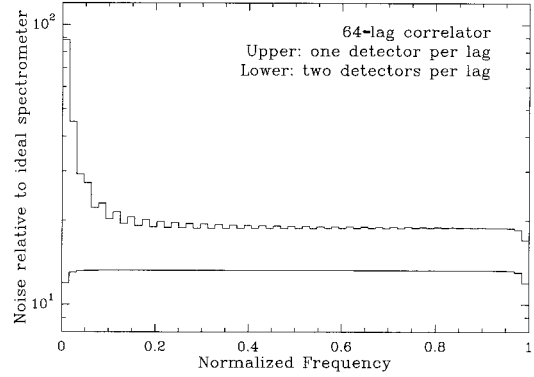


Fig. 6. Comparison of the noise in the spectral channels in the low- $n_0$  limit for 64-lag direct-detection correlators that utilize one (upper line) and two (lower line) detectors per lag.

two-detector configuration, the overall response function of detector  $i$  is given by

$$|S_{i0}(\nu)|^2 = \frac{1}{N_{\text{lags}}} \begin{cases} \cos^2(\pi\delta t_l\nu) & \text{for } i \text{ odd} \\ \sin^2(\pi\delta t_l\nu) & \text{for } i \text{ even} \end{cases}, \quad (81)$$

where  $l$  is the lag index corresponding to detector  $i$ :  $l = \text{int}[(i + 1)/2]$ . For the single-detector configuration, the  $\sin^2(x)$  response functions are omitted, and now  $l = i$ . Using these response functions, the integrals in Eqs. (66) and (70) can be calculated; we chose to use spectral channels with constant width  $\Delta\nu_c = 1/(2\Delta tN_{\text{chan}})$ .

We take a flat input spectrum,  $\lambda_c = \lambda_0$ , which implies a constant input occupation number  $\bar{n}_c = n_0$ . Using Eqs. (69) and (74), the covariance matrix of the estimated spectrum can be written as

$$C^{(\lambda)} = AC^{(D)}A^T = \lambda_0(C^{\text{Pois}} + n_0C^{\text{class}}), \quad (82)$$

where the Poisson noise contribution is given by

$$C_{cc'}^{\text{Pois}} = \sum_i A_{ci} \left( \sum_{c''} p_{ic''} \right) A_{c'i}, \quad (83)$$

whereas the classical noise contribution is

$$C_{cc'}^{\text{class}} = \sum_{ij} A_{ci} \left( \sum_{c''} p_{ic''} P_{j c''} P_{ij c''} \right) A_{c'j}. \quad (84)$$

The variance of spectral channel  $c$  is given by the diagonal element  $C_{cc}^{(\lambda)}$  and can be compared with the variance that would be obtained with an ideal instrument (with  $P = I$ ):

$$C_{cc}^{(\text{ideal})} = \lambda_0(1 + n_0). \quad (85)$$

Figure 6 shows the results of the calculation in the low- $n_0$  limit, when Poisson noise dominates. For this example, we have assumed  $N_{\text{chan}} = N_{\text{lags}} = 64$ ; the results for correlators with one and two detectors per lag are compared. The noise in the spectral channels is normalized to the ideal case [Eq. (85)]; the vertical axis is the relative noise,  $(C_{cc}^{\text{Pois}}/C_{cc}^{\text{ideal}})^{1/2}$ . One immediately observes that the sensitivity of the two-detector correlator is superior, by approximately

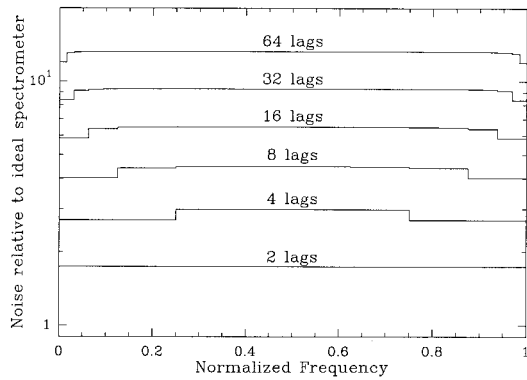


Fig. 7. Variation of the spectral noise in the low- $n_0$  limit as a function of the number of lags. The number of spectral channels is equal to the number of lags, and two detectors are used per lag. The nearly constant spacing between traces indicates that the noise varies as  $\sqrt{N_{\text{lags}}}$ .

$\sqrt{2}$ , but that both are far worse than an ideal (grating) spectrometer. The  $\sqrt{2}$  factor can easily be understood—the two-detector version detects twice as many photons. Also, the noise in the one-detector correlator degrades badly at low frequencies. This behavior is related to the fact that the set of detector response functions is not symmetric with respect to the center of the band when only one detector per lag is used. However, in the classical limit  $n_0 \gg 1$ , the calculation shows that both versions of the correlator give the same sensitivity.

The effect of increasing the number of lags (to obtain higher spectral resolution) is shown in Fig. 7 for the two-detector correlator in the Poisson limit. Again, we have chosen  $N_{\text{chan}} = N_{\text{lags}}$ . This graph demonstrates that the relative sensitivity degrades as  $\sqrt{N_{\text{lags}}}$ . This sensitivity degradation cannot be recovered by decreasing the resolution in the spectrum. Figure 8 shows the effect of reducing  $N_{\text{chan}}$  while keeping  $N_{\text{lags}} = 64$  constant. As can be seen, the noise improvement is marginal. The reason is clear: when  $N_{\text{chan}} < N_{\text{lags}}$ , the extra lags  $l > N_{\text{chan}}$  with large delays  $\delta t_l$  are not needed to recover the spectrum at the resolution dictated by  $N_{\text{chan}}$ , but

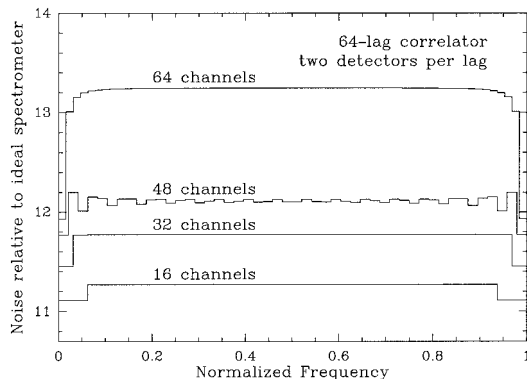


Fig. 8. Variation of the spectral noise in the low- $n_0$  limit for a 64-lag, two-detector correlator as a function of the number of channels in the output spectrum.

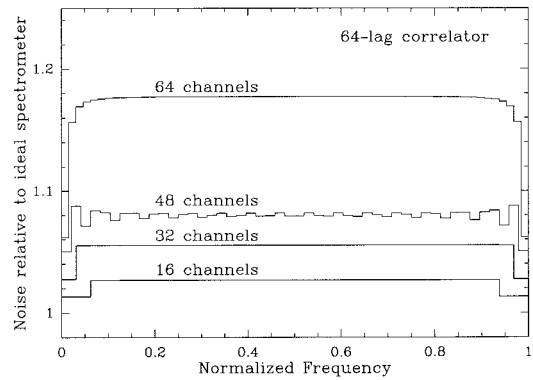


Fig. 9. Variation of the spectral noise in the high- $n_0$  (classical) limit for a 64-lag, two-detector correlator, as a function of the number of channels in the output spectrum.

these extra lags still receive photons. The sensitivity can be improved by removing the unneeded lags and sending more photons to the lags that are useful.

The classical  $n_0 \gg 1$  limit is also of interest. Figure 9 shows the results for a 64-lag correlator at various spectral resolutions given by  $N_{\text{chan}}$ . As can be seen, all the sensitivities are near unity, indicating that the noise in the spectrum closely approaches the noise one would obtain in an ideal filter bank (or grating) spectrometer. The slight improvement in sensitivity with decreasing  $N_{\text{chan}}$  is basically a noise-bandwidth effect: at lower spectral resolution, the frequency response of a channel in the output spectrum is a closer match to a perfect rectangular shape.

Finally, Fig. 10 shows a plot of the relative noise of a spectral channel in the center of the band as a function of photon occupation number  $n_0$  at the spectrometer input. Again, we assume  $N_{\text{chan}} = N_{\text{lags}} = 64$ . We see a gradual transition, over approximately two decades in  $n_0$ , in which the relative noise decreases from the Poisson limit to the near-unity classical limit (note that the actual noise increases with

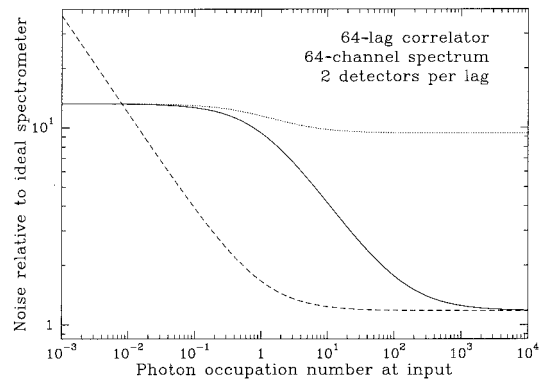


Fig. 10. Solid curve: the variation of the mid-band spectral noise [Eq. (82)] relative to an ideal instrument [Eq. (85)] for a 64-lag, two-detector correlator, producing a 64-channel spectrum, as a function of the photon occupation number at the input. Dashed curve: relative noise for the same correlator, now preceded by a high-gain quantum-limited amplifier [Eq. (86)]. Dotted curve: relative noise for a two-detector FTS [Eq. (88)].

$n_0$ ). The noise is nearly at the classical value when  $n_0 \sim 128$ ; this corresponds to an occupation number of order unity for the mode arriving at the detectors. In the transition region,  $1 < n_0 < N_{\text{det}}$ , the relative noise scales as  $1/\sqrt{n_0}$ , because the noise of the ideal spectrometer is being degraded by photon bunching. The performance of the correlator for  $n_0 \sim 1$  can be improved by use of an amplifier. For a correlator preceded by a high-gain quantum-limited amplifier [see Eq. (49)], the spectral noise (referred to the amplifier input) is given by

$$C^{(\lambda)}(\text{amp}) = C^{\text{class}} \lambda_0 (1 + n_0)(1 + n_0^{-1}), \quad (86)$$

which shows that nearly ideal performance can be obtained for  $n_0 > 1$ ; however, the performance degrades for  $n_0 < 1$ . This result is plotted in Fig. 10; the addition of the amplifier improves the performance for  $n_0 > 1/(2N_{\text{lags}})$ .

#### G. Relationship to a Fourier-Transform Spectrometer

The correlation spectrometer I have described is related to a Fourier-transform spectrometer (FTS) that uses a single interferometer with a moving mirror to measure the correlation function in a time-serial fashion. In fact, we can imagine that we split up the total integration time  $\tau$  into  $N_{\text{lags}}$  sessions, and, over the course of these sessions, the path-length delay of the FTS is stepped over the same values  $\delta t_l$  that are used in the correlator. For a single-detector (Michelson) FTS, the probability that a photon at frequency  $\nu$  that entered the FTS at some point during integration time  $\tau$  is detected when the path-length difference is set to  $\delta t_l$  is

$$p_l(\nu) = \frac{1}{N_{\text{lags}}} \cos^2(\pi \nu \delta t_l). \quad (87)$$

The factor  $1/N_{\text{lags}}$  accounts for the fraction of time that the path-length difference is actually  $\delta t_l$ , whereas the  $\cos^2(x)$  factor gives the frequency response of the detector at that setting. These expressions can readily be generalized to the case of a two-detector (Mach-Zehnder) FTS; the second detector has a  $\sin^2(x)$  response. Thus, the FTS and the correlation spectrometer have identical photon detection probability matrices.<sup>7</sup> As a result, their sensitivities are identical in the low- $n_0$  Poisson regime.

For the strong background case  $n_0 \gg 1$ , the multilag correlator obtains better sensitivity than the scanned FTS, which can measure only one correlation product at a time. This is why radio astronomers spend large sums to build correlators. The principal difference is that the integration time per lag is a factor of  $N_{\text{lags}}$  shorter, which increases the noise by  $\sqrt{N_{\text{lags}}}$ , according to the Dicke equation. Another difference is that the FTS cannot have any correlations between the detector outputs for different path-length settings  $\delta t_l$ , since these readings are obtained at different times. The overall result for the noise in the FTS spectrum is

$$C^{(\lambda)}(\text{FTS}) = \lambda_0 [C^{\text{Pois}} + n_0 C^{\text{class}}(\text{FTS})], \quad (88)$$

where  $C^{\text{Pois}}$  is still given by Eq. (83), but now

$$C_{cc'}^{\text{class}}(\text{FTS}) = N_{\text{lags}} \sum_l \sum_{i \in l} \sum_{j \in l} A_{ci} \left( \sum_{c''} p_{ic''} p_{jc''} \rho_{ijc''} \right) A_{c'j}, \quad (89)$$

and  $p_{ic}$  and  $\rho_{ijc}$  are the same quantities as for the correlator. Index  $l$  labels the lags, i.e., the positions of the moving mirror; the notation  $i, j \in l$  reminds us that the detector indices must be restricted to those that correspond to a given mirror position  $l$  since the detector noise for different positions is uncorrelated. This result is plotted in Fig. 10 for a two-detector FTS.

## 6. Conclusions

The effect of fluctuating thermal radiation backgrounds on the sensitivity of photon detection instruments has been discussed in detail, and a general theory has been presented that can accommodate arbitrary numbers of inputs and detectors and is valid for arbitrary photon occupation numbers  $n$ . The key results, Eqs. (29) and (36), allow us to calculate not only the photon fluctuations for individual detectors but also the correlation of these fluctuations among different detectors. These general results have been applied in a number of special cases and have been shown to reproduce standard results, such as photon shot noise in the  $n \ll 1$  limit [Eq. (47)], and classical thermal noise in the  $n \gg 1$  limit [Eq. (46)]. The sensitivity of multimode detectors, which has been debated in the literature, was discussed in detail and a general sensitivity expression [Eq. (55)] was derived. I have shown that the standard expressions for the sensitivity of multimode detectors are based on certain assumptions, and that our general result can reproduce the standard expressions under the appropriate conditions.

I have analyzed correlation spectrometers in detail and have shown that their sensitivity is degraded (compared with ideal dispersive spectrometers) in the low-background case ( $n \ll 1$ ) but not in the high-background case ( $n \gg 1$ ). The physical interpretation is straightforward. For  $n \ll 1$ , the photons arrive one at a time, and it is important to extract the necessary information from each photon. The grating spectrometer accomplishes this task, since a detection event identifies the photon wavelength to within the desired resolution. This is not true for the correlation spectrometer, which explains the sensitivity penalty. However, when  $n \gg 1$ , the photons arrive in bunches, and therefore produce many correlated detection events. This allows us to reconstruct the wavelength of the bunch by use of information from all the detectors, and so the sensitivity penalty disappears. This example is analogous to the situation for imaging with pairwise-combined spatial interferometers.<sup>7</sup>

### Appendix A: Spatial Modes

In this paper the term modes is used in the standard microwave engineering sense,<sup>71</sup> to distinguish fields

that propagate as traveling waves in some direction but have different transverse field patterns. Such modes obey an orthogonality condition over a surface. Examples include transmission line, waveguide, and optical fiber modes, such as the familiar  $TE_{mn}$  and  $TM_{mn}$  modes for rectangular waveguides, as well as free-space modes, such as the Gauss–Hermite modes. The electric and magnetic multipole fields<sup>72,73</sup> with vector spherical harmonic angular functions and spherical Hankel radial functions are another example and obey an orthogonality condition over the surface of a sphere. The propagation direction for this case is interpreted to mean toward or away from the origin  $r = 0$ . In all cases, the modes are labeled by one or more discrete indices, such as the  $(m, n)$  indices for rectangular waveguides. The modes are also indexed by frequency, which is a continuous variable. In essence, the concept of a mode as used in this paper amounts to a specification of the form of the incoming or outgoing electromagnetic fields in the asymptotic region, before or after interactions with the optical system. For scattering problems, the term channel is sometimes used instead<sup>53</sup> to describe this concept.

## Appendix B: Definition of Classical Wave Amplitudes and Quantum Operators

### 1. Normalization of the Classical Amplitudes

The definition of the classical wave amplitudes and the corresponding quantum (photon) operators is most easily understood within the context of an ideal single-mode transmission line, which is the case we discuss here. The case of multimode waveguides is formally equivalent to a set of independent single-mode transmission lines,<sup>71</sup> and the electromagnetic fields inside the waveguide can be expressed in terms of equivalent voltages and currents on the transmission lines. The definition of wave amplitudes and quantum operators for general open electromagnetic scattering systems has been discussed recently,<sup>53</sup> as has the quantization of the multipole modes.<sup>73</sup>

The equations of motion for voltage  $V_i$  and current  $I_i$  on an ideal transmission line are

$$\frac{\partial V_i(x, t)}{\partial x} = -\mathcal{L} \frac{\partial I_i(x, t)}{\partial t}, \quad (\text{B1})$$

$$\frac{\partial I_i(x, t)}{\partial x} = -\mathcal{C} \frac{\partial V_i(x, t)}{\partial t}, \quad (\text{B2})$$

where  $\mathcal{L}$  and  $\mathcal{C}$  are the inductance and the capacitance per unit length, respectively. These equations have traveling-wave solutions of the form  $\exp(j2\pi\nu t \pm jkx)$ , where  $k = 2\pi\nu/\bar{c}$ , and  $\bar{c} = 1/\sqrt{\mathcal{L}\mathcal{C}}$  is the phase velocity. Accordingly, we can write the solutions for voltage and current as superpositions of these traveling waves,

$$V_i(x, t) = \sqrt{\frac{Z_0}{2}} \int_0^\infty d\nu \exp(+j2\pi\nu t) [a_i(\nu) \exp(-jkx) + b_i(\nu) \exp(+jkx)] + \text{c.c.} \quad (\text{B3})$$

where  $a_i(\nu)$  is the amplitude of the forward wave,  $b_i(\nu)$  is the amplitude of the reverse wave,  $Z_0 = \sqrt{\mathcal{L}/\mathcal{C}}$  is the characteristic impedance, and c.c. is the complex conjugate of the preceding expression. Similarly,

$$I_i(x, t) = \frac{1}{\sqrt{2Z_0}} \int_0^\infty d\nu \exp(+j2\pi\nu t) [a_i(\nu) \times \exp(-jkx) - b_i(\nu) \exp(+jkx)] + \text{c.c.} \quad (\text{B4})$$

The total energy on the line is given by the sum of the electric and magnetic contributions

$$U_i(t) = \int_{-\infty}^{+\infty} dx \left[ \frac{1}{2} \mathcal{C} V_i^2(x, t) + \frac{1}{2} \mathcal{L} I_i^2(x, t) \right] \quad (\text{B5})$$

and can be evaluated in terms of the wave amplitudes as

$$U_i = \int_0^\infty d\nu |a_i(\nu)|^2 + |b_i(\nu)|^2, \quad (\text{B6})$$

which is seen to be time independent, as expected since the system has no dissipation. The simple form of this expression motivates our chosen normalization of the wave amplitudes.

By taking Fourier transforms, we can write

$$a_i(\nu) = \int_{-\infty}^{+\infty} dt \exp(-j2\pi\nu t) \times \frac{V_i(0, t) + Z_0 I_i(0, t)}{\sqrt{2Z_0}}, \quad (\text{B7})$$

$$b_i(\nu) = \int_{-\infty}^{+\infty} dt \exp(-j2\pi\nu t) \times \frac{V_i(0, t) - Z_0 I_i(0, t)}{\sqrt{2Z_0}}, \quad (\text{B8})$$

where we have arbitrarily chosen  $x = 0$  as our reference plane to connect the wave amplitudes to the voltage and current. Thus, wave amplitudes  $a_i(\nu)$  and  $b_i(\nu)$  can be regarded as Fourier transforms of the corresponding time-domain quantities  $a_i(t)$  and  $b_i(t)$ .

### 2. Monochromatic Radiation

For perfectly monochromatic radiation at frequency  $\nu_0$ , traveling in the forward direction only, we would write

$$a_i(\nu) = a_i \delta(\nu - \nu_0). \quad (\text{B9})$$

According to Eq. (B6), the total energy stored on the line in this case is infinite, which is expected since the wave amplitude and therefore the energy per unit length is constant along the line. On the other hand,

the power carried by the wave is finite. The voltage and current at  $x = 0$  are

$$V_i(0, t) = \sqrt{2Z_0} \operatorname{Re}[a_i \exp(+j2\pi\nu t)], \quad (\text{B10})$$

$$I_i(0, t) = \sqrt{\frac{2}{Z_0}} \operatorname{Re}[a_i \exp(+j2\pi\nu t)], \quad (\text{B11})$$

from which we calculate the time-averaged power

$$P_i = \langle I_i(0, t)V_i(0, t) \rangle_t = |a_i|^2. \quad (\text{B12})$$

Thus, our chosen normalization of the wave amplitudes also yields a simple result for the power of a monochromatic signal.

### 3. Incoherent Radiation

For incoherent radiation,  $a_i(t)$  is a stationary random process, and it is well known that the Fourier-transform integral for  $a_i(\nu)$  does not converge in the usual mathematical sense. Nevertheless,  $a_i(\nu)$  can be considered to be a complex random quantity with a generalized correlation function

$$\langle a_i(\nu)a_i^*(\nu') \rangle = A_i(\nu)\delta(\nu - \nu'), \quad (\text{B13})$$

where  $A_i(\nu)$ , the spectral density of  $a_i(t)$ , represents the noise power per unit bandwidth. Both monochromatic and noise signals can be treated in a unified fashion by introducing the definition

$$\begin{aligned} a_i &= \int_{\nu_0 - \Delta\nu/2}^{\nu_0 + \Delta\nu/2} d\nu a_i(\nu) \\ &= \int_{-\infty}^{+\infty} a_i(t) \exp(-j2\pi\nu_0 t) \operatorname{sinc}(\pi\Delta\nu t) \Delta\nu, \end{aligned}$$

which clearly agrees with the previous definition of  $a_i$  for the monochromatic case. For incoherent radiation,  $a_i$  represents the (random) complex noise amplitude in bandwidth  $\Delta\nu$  about frequency  $\nu_0$  and is mathematically well defined in terms of  $a_i(t)$ . The mean-square value of  $a_i$  is finite,  $\langle |a_i|^2 \rangle = A_i(\nu_0)\Delta\nu$ , and represents the power within the bandwidth  $\Delta\nu$ . This approach is common in electrical engineering [see Eqs. (3) and (4)].

### 4. Relationship of Classical Amplitudes and Quantum Operators

Electrical engineers represent time-harmonic behavior by use of  $\exp(j\omega t)$  whereas physicists use  $\exp(-i\omega t)$ . Quantum optics, which intimately combines concepts from both fields, offers us many opportunities to confuse these two definitions. Our point of view is that the numerical values of the scattering matrix elements  $S_{ij}(\nu)$  should be the same for the classical and quantum mechanical cases and that the definition of the scattering matrix should follow the standard usage in electrical (microwave) engineering. Not all researchers adopt this convention, and sometimes Eq. (7) is written in terms of photon destruction operators, in which case the classical and quantum scattering matrices are complex conjugates

of each other. We define the scattering matrix by the equation relating incoming and outgoing classical (engineering) wave amplitudes,

$$b_i(\nu) = \sum_j S_{ij}(\nu)a_j(\nu), \quad (\text{B14})$$

where for simplicity we assume that the scattering matrix is unitary and no noise terms are needed. For a transmission line that carries only forward waves with amplitudes  $a_{cl}(\nu)$ , the classical voltage is given by

$$\begin{aligned} V_{cl}(x, t) &= \sqrt{\frac{Z_0}{2}} \int_0^\infty d\nu [a_{cl}(\nu) \exp(+j2\pi\nu t) \exp(-jkx) \\ &\quad + a_{cl}^*(\nu) \exp(-j2\pi\nu t) \exp(+jkx)]. \end{aligned} \quad (\text{B15})$$

For the quantum-mechanical case, we would write a similar expression for the voltage operator in the Heisenberg picture for the forward waves:

$$\begin{aligned} V_{op}(x, t) &= \sqrt{\frac{Z_0}{2}} \int_0^\infty d\nu \sqrt{\hbar\nu} [a(\nu) \\ &\quad \times \exp(-i2\pi\nu t) \exp(+ikx) \\ &\quad + a^\dagger(\nu) \exp(+i2\pi\nu t) \exp(-ikx)], \end{aligned} \quad (\text{B16})$$

where now  $a(\nu)$  and  $a^\dagger(\nu)$  are photon destruction and creation operators, respectively. The time dependence differs from the classical expression but follows standard usage in quantum mechanics<sup>43</sup> and is consistent with the Heisenberg equation of motion,

$$i\hbar \frac{\partial a(t)}{\partial t} = [a(t), H], \quad (\text{B17})$$

for the case of a simple harmonic oscillator with Hamiltonian  $H = \hbar\omega a^\dagger a$ .

The connection between the classical voltage [Eq. (B15)] and the quantum voltage operator [Eq. (B16)] is made by supposing that the excitation of the transmission line can be described by a quantum-mechanical coherent state,  $|\psi\rangle = |\alpha(\nu)\rangle$ . For this state, the expectation values of the photon operators are

$$\begin{aligned} \langle a(\nu) \rangle &= \langle \psi | a(\nu) | \psi \rangle = \alpha(\nu), \\ \langle a^\dagger(\nu) \rangle &= \langle \psi | a^\dagger(\nu) | \psi \rangle = \alpha^*(\nu). \end{aligned}$$

To make the expectation value of the quantum voltage operator  $\langle V_{op}(x, t) \rangle$  match the classical expression Eq. (B15), we must have

$$a_{cl}^*(\nu) = \alpha(\nu) \sqrt{\hbar\nu}. \quad (\text{B18})$$

The classical scattering equation [Eq. (B14)], when the incoming waves are described by coherent states  $|\alpha_j(\nu)\rangle$ , can be written as

$$\beta_i^*(\nu) = \sum_j S_{ij}(\nu) \alpha_j^*(\nu), \quad (\text{B19})$$

since we realize that the outgoing waves should also be described by coherent states  $|\beta_i(\nu)\rangle$ . Note that  $S_{ij}(\nu)$  in Eq. (B19) is the classical scattering matrix. However, since this result is just the expectation value of Eq. (7) involving the quantum operators, we see that the classical and quantum scattering matrices are in fact identical given our choice of definitions.

### Appendix C: Operator Averages in Thermal Equilibrium

In this Appendix I derive the various thermal averages of photon and noise operators that were needed in Section 2. The results presented here are well known; they are listed for completeness and to indicate an elementary method of derivation.

Note that the average of some physical quantity  $A$  can be calculated in quantum statistical mechanics by taking the trace over the density operator  $\rho$ :

$$\langle A \rangle = \text{Tr}(\rho A). \quad (\text{C1})$$

For a single incoming photon mode, described by the operator  $a_i(\nu)$ , the density operator in thermal equilibrium is

$$\rho_i = C_i \exp\left[-\int d\nu \frac{h\nu N_i(\nu)}{kT_i}\right], \quad (\text{C2})$$

where  $N_i(\nu) = a_i^\dagger(\nu)a_i(\nu)$  is the photon number density operator. The normalization constant  $C_i$  is chosen so that  $\text{Tr}(\rho_i) = 1$ . If we have multiple modes, the overall density matrix is simply the product of the density matrices for each mode,

$$\rho = \prod_i \rho_i, \quad (\text{C3})$$

since the incoming modes are independent and uncorrelated, by assumption. It is not difficult to show from the commutation relations that the rule for interchanging the order of operators  $\rho_i$  and  $a_i$  is

$$\rho_i a_i(\nu) = \exp(h\nu/kT_i) a_i(\nu) \rho_i. \quad (\text{C4})$$

#### 1. Products of Two Photon Operators

We are now ready to calculate the average of a product of two-photon operators:

$$\begin{aligned} \langle a_i^\dagger(\nu) a_j(\nu') \rangle &= \text{Tr}[\rho a_i^\dagger(\nu) a_j(\nu')] \\ &= \text{Tr}[\rho a_j(\nu') a_i^\dagger(\nu)] \\ &\quad - \text{Tr}\{\rho [a_j(\nu'), a_i^\dagger(\nu)]\} \\ &= \exp(h\nu'/kT_j) \text{Tr}[a_j(\nu') \rho a_i^\dagger(\nu)] \\ &\quad - \text{Tr}(\rho) \delta_{ij} \delta(\nu - \nu') \\ &= \exp(h\nu'/kT_j) \langle a_i^\dagger(\nu) a_j(\nu') \rangle \\ &\quad - \delta_{ij} \delta(\nu - \nu'), \end{aligned}$$

where for the last step we used the cyclic property of the trace and also  $\text{Tr}(\rho) = 1$ . Solving for the expectation value,

$$\begin{aligned} \langle a_i^\dagger(\nu) a_j(\nu') \rangle &= \delta_{ij} \delta(\nu - \nu') [\exp(h\nu/kT_i) - 1]^{-1} \\ &= n_{\text{th}}(\nu, T_i) \delta_{ij} \delta(\nu - \nu'). \quad (\text{C5}) \end{aligned}$$

Here  $n_{\text{th}}(\nu, T)$  is recognized as the Bose–Einstein distribution function (mean occupancy) for a single mode at a temperature  $T$ . A similar calculation demonstrates that the averages of two destruction or two creation operators vanish, as expected:

$$\langle a_i(\nu) a_j(\nu') \rangle = 0 = \langle a_i^\dagger(\nu) a_j^\dagger(\nu') \rangle. \quad (\text{C6})$$

#### 2. Products of Four Photon Operators

We also need the average of four-photon operators, which we can obtain by again cycling the rightmost photon operator to the left, past the other operators. A straightforward calculation gives

$$\begin{aligned} \langle a_i^\dagger(\nu_1) a_j(\nu_2) a_k^\dagger(\nu_3) a_l(\nu_4) \rangle &= n_{\text{th}}(\nu_1, T_i) (n_{\text{th}}(\nu_3, T_k) \\ &\quad + 1) \delta_{il} \delta_{jk} \delta(\nu_1 - \nu_4) \delta(\nu_2 - \nu_3) \\ &\quad + n_{\text{th}}(\nu_1, T_i) n_{\text{th}}(\nu_3, T_k) \delta_{ij} \delta_{kl} \delta(\nu_1 - \nu_2) \delta(\nu_3 - \nu_4). \quad (\text{C7}) \end{aligned}$$

#### 3. Correlation of Four Noise Operators

Equation (18) gives the result for the noise correlation matrix  $C_{ij}(\nu)$ , which provides the correlation of two noise operators:

$$\langle c_i^\dagger(\nu) c_j(\nu') \rangle = C_{ij}(\nu) \delta(\nu - \nu'). \quad (\text{C8})$$

All higher-order correlations can be calculated in terms of  $C_{ij}(\nu)$  and the scattering matrix  $S_{ij}(\nu)$ . For example, the correlation of four noise operators can be found by use of Eq. (C7):

$$\begin{aligned} \langle c_i^\dagger(\nu_1) c_j(\nu_2) c_k^\dagger(\nu_3) c_l(\nu_4) \rangle &= \sum_{\alpha, \beta, \gamma, \delta} S_{i\alpha}'(\nu_1) S_{j\beta}'^*(\nu_2) S_{k\gamma}'(\nu_3) S_{l\delta}'^*(\nu_4) \\ &\quad \times \langle a_\alpha^\dagger(\nu_1), a_\beta(\nu_2) a_\gamma^\dagger(\nu_3), a_\delta(\nu_4) \rangle \\ &= \sum_{\alpha, \gamma} S_{i\alpha}'(\nu_1) S_{l\alpha}'^*(\nu_4) n_{\text{th}}(\nu_1, T_\alpha) S_{k\gamma}'(\nu_3) S_{j\gamma}'^*(\nu_2) \\ &\quad \times [n_{\text{th}}(\nu_3, T_\gamma) + 1] \delta(\nu_1 - \nu_4) \delta(\nu_3 - \nu_2) \\ &\quad + S_{i\alpha}'(\nu_1) S_{j\alpha}'^*(\nu_2) n_{\text{th}}(\nu_1, T_\alpha) S_{l\gamma}'^*(\nu_3) S_{k\gamma}'(\nu_3) \\ &\quad \times n_{\text{th}}(\nu_3, T_\gamma) \delta(\nu_1 - \nu_2) \delta(\nu_3 - \nu_4). \end{aligned}$$

Applying the definition of the noise correlation matrix given in Eq. (18) as well as the relation in Eq. (14), we can express our result as

$$\begin{aligned} \langle c_i^\dagger(\nu_1) c_j(\nu_2) c_k^\dagger(\nu_3) c_l(\nu_4) \rangle &= \delta(\nu_1 - \nu_4) \\ &\quad \times \delta(\nu_3 - \nu_2) C_{il}(\nu_1) \{C_{kj}(\nu_3) \\ &\quad + [\mathbf{1} - \mathbf{S}(\nu_3) \mathbf{S}^\dagger(\nu_3)]_{kj}\} \\ &\quad + \delta(\nu_1 - \nu_2) \delta(\nu_3 - \nu_4) C_{ij}(\nu_1) C_{kl}(\nu_3). \quad (\text{C9}) \end{aligned}$$

It is readily seen that Eqs. (C7) and (C9) could have been obtained more easily by first applying the commutation relations to move  $a_k^\dagger$  or  $c_k^\dagger$  to the left (to normal order) and then combining the creation and destruction operators in pairs to obtain two terms of the form  $\langle c_i^\dagger c_j \rangle \langle c_k^\dagger c_l \rangle$  and  $\langle c_i^\dagger c_j \rangle \langle c_k^\dagger c_j \rangle$ . This is a general technique that is applicable for the calculation of

thermal averages of products of arbitrary numbers of photon operators.

The author thanks J. Bock, H. Moseley, T. G. Phillips, R. Schieder, and R. Schoelkopf for helpful discussions and comments. This study was supported in part by NASA grant NAG5-8589 to Yale University, subcontract Y-99-0019 to Caltech. The author is grateful for the generous support of Alex Lidow, a Caltech Trustee.

## References and Notes

1. R. H. Dicke, "The measurement of thermal radiation at microwave frequencies," *Rev. Sci. Instrum.* **17**, 268–275 (1946).
2. R. Hanbury Brown and R. Q. Twiss, "Correlation between photons in 2 coherent beams of light," *Nature* **177**, 27–29 (1956).
3. R. Nityananda, "Comparing optical and radio – quantum issues," in *Very High Resolution Angular Imaging: Proceedings of the International Astronomical Union*, J. G. Robertson and W. J. Tango, eds. (Kluwer Academic, Dordrecht, The Netherlands, 1994), pp. 11–18.
4. M. Kamionkowski and A. H. Jaffe, "Detection of gravitational waves from inflation," *Int. J. Mod. Phys. A (Suppl. 1A)* **16**, 116–128 (2001).
5. C. M. Caves, "Quantum limits on noise in linear amplifiers," *Phys. Rev. D* **26**, 1817–1839 (1982).
6. S. Prasad, "Implications of light amplification for astronomical imaging," *J. Opt. Soc. Am. A* **11**, 2799–2803 (1994).
7. J. Zmuidzinas, "Cramér–Rao sensitivity limits for astronomical instruments: implications for interferometer design," *J. Opt. Soc. Am. A* **20**, 218–233 (2003).
8. J. M. W. Milatz and H. A. van der Velden, "Natural limit of measuring radiation with a bolometer," *Physica* **10**, 369–380 (1943).
9. W. B. Lewis, "Fluctuations in streams of thermal radiation," *Proc. Phys. Soc.* **59**, 34–40 (1947).
10. M. J. E. Golay, "Theoretical consideration in heat and infra-red detection, with particular reference to the pneumatic detector," *Rev. Sci. Instrum.* **18**, 347–356 (1947).
11. R. C. Jones, "The ultimate sensitivity of radiation detectors," *J. Opt. Soc. Am.* **37**, 879–890 (1947).
12. P. B. Felgett, "On the ultimate sensitivity and practical performance of radiation detectors," *J. Opt. Soc. Am.* **39**, 970–976 (1949).
13. P. Felgett, R. C. Jones, and R. Q. Twiss, "Fluctuations in photon streams," *Nature* **184**, 967–969 (1959).
14. C. W. McCombie, "Fluctuations in photon streams," *Nature* **184**, 969–970 (1959).
15. K. M. vanVliet, "Noise limitations in solid-state photodetectors," *Appl. Opt.* **6**, 1145–1169 (1967).
16. J. C. Mather, "Bolometer noise: nonequilibrium theory," *Appl. Opt.* **21**, 1125–1129 (1982).
17. R. W. Boyd, "Photon bunching and the photon-noise-limited performance of infrared detectors," *Infrared Phys.* **22**, 157–162 (1982).
18. J. M. Lamarre, "Photon noise in photometric instruments at far-infrared and submillimeter wavelengths," *Appl. Opt.* **25**, 870–876 (1986).
19. P. L. Richards, "Bolometers for infrared and millimeter waves," *J. Appl. Phys.* **76**, 1–24 (1994).
20. D. Benford, T. Hunter, and T. Phillips, "Noise equivalent power of background limited thermal detectors at submillimeter wavelengths," *Int. J. Infrared Millim. Waves* **19**, 931–938 (1998).
21. G. A. Rebka and R. V. Pound, "Time-correlated photons," *Nature* **180**, 1035–1036 (1957).
22. M. Harwit, "Measurement of thermal fluctuations in radiation," *Phys. Rev.* **120**, 1551–1556 (1960).
23. B. L. Morgan and L. Mandel, "Measurement of photon bunching in a thermal light beam," *Phys. Rev. Lett.* **16**, 1012–1015 (1966).
24. R. Hanbury Brown and R. Q. Twiss, "The question of correlation between photons in coherent light rays," *Nature* **178**, 1447–1448 (1956).
25. E. M. Purcell, "The question of correlation between photons in coherent light rays," *Nature* **178**, 1449–1450 (1956).
26. R. Hanbury Brown and R. Q. Twiss, "Interferometry of the intensity fluctuations in light: I. Basic theory: the correlation between photons in coherent beams of radiation," *Proc. R. Soc. London Ser. A* **242**, 300–324 (1957).
27. P. Felgett, "The question of correlation between photons in coherent beams of light," *Nature* **179**, 956–957 (1957).
28. R. Q. Twiss and R. Hanbury Brown, "The question of correlation between photons in coherent beams of light," *Nature* **179**, 1128–1129 (1957).
29. R. M. Sillitto, "Correlation between events in photon detectors," *Nature* **179**, 1127–1128 (1957).
30. R. J. Glauber, "The quantum theory of optical coherence," *Phys. Rev.* **130**, 2529–2539 (1963).
31. L. Mandel and E. Wolf, "Coherence properties of optical fields," *Rev. Mod. Phys.* **37**, 231–287 (1965).
32. V. V. Karavaev, "Output fluctuations of thermal radiation detectors," *Sov. Phys. JETP* **22**, 570–577 (1966).
33. J. B. Johnson, "Thermal agitation of electricity in conductors," *Phys. Rev.* **32**, 97–109 (1928).
34. H. Nyquist, "Thermal agitation of electric charge in conductors," *Phys. Rev.* **32**, 110–113 (1928).
35. H. B. Callen and T. A. Welton, "Irreversibility and generalized noise," *Phys. Rev.* **83**, 34–40 (1951).
36. H. Bosma, "On the theory of linear noisy systems," *Philips Res. Rep. Suppl.* **10**, 1–190 (1967).
37. J. Murphy, S. Withington, and A. Egan, "Mode conversion at diffracting apertures in millimeter and submillimeter-wave optical-systems," *IEEE Trans. Microwave Theory Tech.* **41**, 1700–1702 (1993).
38. J. Murphy and S. Withington, "Perturbation analysis of Gaussian-beam-mode scattering at off-axis ellipsoidal mirrors," *Infrared Phys. Technol.* **37**, 205–219 (1996).
39. S. Withington and J. Murphy, "Modal analysis of partially coherent submillimeter-wave quasi-optical systems," *IEEE Trans. Antennas Propag.* **46**, 1651–1659 (1998).
40. D. M. Pozar, *Microwave Engineering*, 2nd ed. (Wiley, New York, 1998).
41. S. W. Wedge and D. B. Rutledge, "Noise waves and passive linear multiports," *IEEE Microwave Guid. Wave Lett.* **1**, 117–119 (1991).
42. H. Haus, "Steady-state quantum analysis of linear systems," *Proc. IEEE* **58**, 1599–1611 (1970).
43. B. Yurke and J. S. Denker, "Quantum network theory," *Phys. Rev. A* **29**, 1419–1437 (1984).
44. H. A. Haus and Y. Yamamoto, "Quantum circuit theory of phase-sensitive linear systems," *IEEE J. Quantum Electron.* **QE-23**, 212–221 (1987).
45. J. R. Jeffers, N. Imoto, and R. Loudon, "Quantum optics of traveling-wave attenuators and amplifiers," *Phys. Rev. A* **47**, 3346–3359 (1993).
46. E. Berglind and L. Gillner, "Optical quantum noise treated with classical electrical network theory," *IEEE J. Quantum Electron.* **30**, 846–853 (1994).
47. R. Matloob, R. Loudon, S. M. Barnett, and J. Jeffers, "Electromagnetic field quantization in absorbing dielectrics," *Phys. Rev. A* **52**, 4823–4838 (1995).
48. T. Gruner and D.-G. Welsch, "Quantum-optical input–output

- relations for dispersive and lossy multilayer dielectric plates,” *Phys. Rev. A* **54**, 1661–1677 (1996).
49. S. M. Barnett, J. Jeffers, A. Gatti, and R. Loudon, “Quantum optics of lossy beam splitters,” *Phys. Rev. A* **57**, 2134–2145 (1998).
  50. C. W. J. Beenakker, “Thermal radiation and amplified spontaneous emission from a random medium,” *Phys. Rev. Lett.* **81**, 1829–1832 (1998).
  51. L. Knöll, S. Scheel, E. Schmidt, D.-G. Welsch, and A. V. Chizhov, “Quantum-state transformation by dispersive and absorbing four-port devices,” *Phys. Rev. A* **59**, 4716–4726 (1999).
  52. S. Savasta, O. Di Stefano, and R. Girlanda, “Light quantization for arbitrary scattering systems,” *Phys. Rev. A* **65**, 043801 (2002); see Eq. (4.28).
  53. C. Viviescas and G. Hackenbroich, “Field quantization for open optical cavities,” *Phys. Rev. A* **67**, 013805 (2003).
  54. K. J. Blow, R. Loudon, S. J. D. Phoenix, and T. J. Shepherd, “Continuum fields in quantum optics,” *Phys. Rev. A* **42**, 4102–4114 (1990).
  55. R. Loudon, *Quantum Theory of Light*, 3rd ed. (Oxford U. Press, New York, 2000), Chap. 6.
  56. R. J. Glauber, “Coherent and incoherent states of the radiation field,” *Phys. Rev.* **131**, 2766–2788 (1963).
  57. P. L. Kelley and W. H. Kleiner, “Theory of electromagnetic field measurement and photoelectron counting,” *Phys. Rev.* **136**, A316–A334 (1964).
  58. B. R. Mollow, “Quantum theory of field attenuation,” *Phys. Rev.* **168**, 1896–1919 (1968).
  59. H. J. Kimble and L. Mandel, “Photoelectric detection of polychromatic light,” *Phys. Rev. A* **30**, 844–850 (1984).
  60. R. S. Bondurant, “Response of ideal photodetectors to photon flux and/or energy flux,” *Phys. Rev. A* **32**, 2797–2802 (1985).
  61. B. Yurke, “Wideband photon counting and homodyne detection,” *Phys. Rev. A* **32**, 311–323 (1985).
  62. S. W. Wedge, “Computer-aided design of low noise microwave circuits,” Ph.D. dissertation (California Institute of Technology, Pasadena, Calif., 1991).
  63. S. W. Wedge and D. B. Rutledge, “Wave techniques for noise modeling and measurement,” *IEEE Trans. Microwave Theory Tech.* **40**, 2004–2012 (1992).
  64. S. W. Wedge and D. B. Rutledge, “Wave computations for microwave education,” *IEEE Trans. Educ.* **36**, 127–131 (1993).
  65. J. Ward, F. Rice, G. Chattopadhyay, and J. Zmuidzinas, “SuperMix: a flexible software library for high-frequency circuit simulation, including SIS mixers and superconducting elements,” in *Tenth International Symposium on Space Terahertz Technology: Symposium Proceedings* (University of Virginia, Charlottesville, Va., 1999), pp. 268–281.
  66. See <http://www.submm.caltech.edu/supermix>.
  67. J. A. Tauber and N. R. Erickson, “A low-cost filterbank spectrometer for submm observations in radio astronomy,” *Rev. Sci. Instrum.* **62**, 1288–1292 (1991).
  68. S. Padin, T. Clark, M. Ewing, R. Finch, R. Lawrence, J. Navarro, S. Scott, N. Scoville, C. Seelinger, and T. Seling, “A high-speed digital correlator for radio astronomy,” *IEEE Trans. Instrum. Meas.* **42**, 793–798 (1993).
  69. M. Torres, “A frequency-agile hybrid spectral correlator for mm-wave radio interferometry,” *Rev. Sci. Instrum.* **65**, 1537–1540 (1994).
  70. A. I. Harris and J. Zmuidzinas, “A wideband lag correlator for heterodyne spectroscopy of broad astronomical and atmospheric spectral lines,” *Rev. Sci. Instrum.* **72**, 1531–1538 (2001).
  71. R. F. Harrington, *Time-Harmonic Electromagnetic Fields*, IEEE Press Series on Electromagnetic Wave Theory (Wiley, New York, 2001), Chap. 8.
  72. J. D. Jackson, *Classical Electrodynamics*, 3rd ed. (Wiley, New York, 1998).
  73. A. Shumovsky, “Quantum multipole radiation,” *Adv. Chem. Phys.* **119**, 395–490 (2001).